Intravital Cell Imaging 法の開発と脳科学への応用：Single Cell の知見のin situ での検証

Intravital Cell Imaging 法の開発と脳科学への応用

－Single Cell の知見の in situ での検証－

（研究課題番号　16390407）

平成１６年度～平成１８年度
科学研究費補助金（基盤研究Ｂ）
研究成果報告書

平成１９年６月

研究代表者　山本清二
（浜松医科大学・光量子医学研究センター・准教授）

はしがき

本研究「Intravital Cell Imaging 法の開発と脳科学への応用—Single Cell の知見の in situ での検証—」は平成１６年度 ～ 平成１８年度　科学研究費補助金（基盤研究Ｂ 研究課題番号 16390407）を受けて行われた。最終年度の終了にあたり研究成果報告をまとめることになった。

研究組織

研究代表者：山本清二（浜松医科大学・光量子医学研究センター・助教授）

研究分担者：寺川　進（浜松医科大学・光量子医学研究センター・教授）

櫻井孝司（浜松医科大学・光量子医学研究センター・助手）

塚田秀夫（浜松ホトニクス㈱・中央研究所・主任部員）

研究協力者：茨木京子（浜松医科大学・光量子医学研究センター・研究員）

王　勇　（浜松医科大学・光量子医学研究センター・大学院生）

山本淳考（浜松医科大学・脳神経外科・大学院生）

研究経費

平成１６年度	４，６００千円
平成１７年度	３，８００千円
平成１８年度	４，５００千円
計	１２，９００千円

はじめに

我々はラット培養神経細胞を用いてグルタミン酸による興奮性神経細胞死の過程を光学顕微鏡、共焦点蛍光顕微鏡、全反射型（エバネッセンス）蛍光顕微鏡で観察し、神経細胞死のメカニズムを解明してきた。その中で、興奮性細胞死の過程で見られる細胞内アシドーシスでは、細胞内のH^+を汲み出す唯一の機構であるNa^+/H^+ exchangerを阻害してもむしろアシドーシスが改善するというparadoxを経験した。これは、Na^+/H^+ exchanger阻害剤がアシドーシスの原因であるミトコンドリア障害を引き起こすCa^{2+}流入を阻害するからであることが分かった（Yamamoto S, Matsumoto Y, Suzuki Y, Tsuboi T, Terakawa S, Ohashi N, Umemura K: An Na^+/H^+ exchanger inhibitor suppresses cellular swelling and neuronal death induced by glutamate in cultured cortical neurons. Acta Neurochir [Supple] 86: 223-226, 2003; Matsumoto Y, Yamamoto S, Suzuki Y, Tsuboi T, Terakawa S, Ohashi N, Umemura K: Na^+/H^+ exchanger inhibitor, SM-20220, is protective against excitotoxicity in cultured cortical neurons. Stroke 35: 185-190, 2004）。この例だけでなく、培養細胞で見られる神経細胞死では細胞内へのCa^{2+}流入がすべてと言ってもいいほど重要な役割を果たしており、逆にこれを阻害する薬剤は神経保護的に働く。しかし、NMDA受容体阻害剤の例のように、これらの薬剤が必ずしも個体レベル(in situ)で保護的かどうかは明らかではない。このように培養細胞と個体レベルでの知見のギャップは未だ大きく、培養細胞を用いた実験の必要性・重要性に疑問の余地はないが、今後の臨床医学を念頭に置いた基礎研究におけるin situ studyの重要性を再認識させられた。この培養細胞と個体レベルでのギャップを検証し埋めることができれば、治療を念頭に置いた基礎研究をさらに発展させることができると考えられる。また近年、遺伝子治療や細胞・組織の移植など、積極的に分子生物学的知見に基づいた治療が実用化に向けて盛んに研究されている。これらの実験的治療が安全かつ確実に臨床に応用されるためにも、遺伝子を導入した細胞や移植した細胞が個体内でどのような振る舞いをするのか

を捉えることが必要不可欠である。

我々は当該科研費を申請する段階で、preliminaryではあるが、ファイバー共焦点顕微鏡、in situ lipofection 法による蛍光蛋白の脳での発現など、Intravital Cell Imaging に必要な手技をいくつか試み、実用レベルに到達しつつあった。本研究ではそれらを応用発展させて、**Intravital Cell Imaging 法を開発**し、これによって**培養細胞（single cell）での知見を in situ で検証、両者のギャップを埋める**ことを試みた。具体的には、我々のところで培養細胞での知見が集積されている「虚血性神経細胞死」をテーマとして選択し、Ca^{2+}シグナル、セカンドメッセンジャーシステム、ミトコンドリア障害、活性酸素、酸化ストレスなどキーワードとする「動物の個体内での虚血性神経細胞死における細胞レベルの反応」を検討することを試みた。

研究期間内に、ラット大脳皮質での脳虚血時における細胞内活性酸素産生のイメージング（Intravital cell imaging of the cerebral cortex upon ischemia-reperfusion in rats）、ラット海馬での脳虚血時における細胞内カルシウムイオン濃度変化のイメージング（Intravital cell imaging of the hippocampus in transient forebrain ischemia in rats）、ラット脳腫瘍での光線力学療法における一重項酸素産生のモニタリング（Monitoring of singlet oxygen for the experimental photodynamic therapy of the glioma in rats）を可能にする成果をあげ、学会発表・論文発表を行った。ここにそれらの成果をまとめ、研究発表リスト、（Ⅰ）Intravital cell imaging of the cerebral cortex upon ischemia-reperfusion in rats、（Ⅱ）Intravital cell imaging of the hippocampus in transient forebrain ischemia in rats、（Ⅲ）Monitoring of singlet oxygen for the experimental photodynamic therapy of the glioma in rats（巻末には、2007年5月20日－24日に大阪市で開催されたthe 23rd International Symposium on Cerebral Blood Flow, Metabolism & Function (Brain' 07) and the 8th International Conference on Quantification of Brain Function with PET (BrainPET' 07)に発表した３演題）を掲載する。

研 究 発 表

(1) 出版物

1-A) 英文

1. Ohkura K, Kazui T, Yamamoto S, Yamashita K, Terada H, Washiyama, N, Suzuki T, Suzuki K, Fujie M, Ohishi K: Comparison of pH management during antegrade selective cerebral perfusion in canine models with old cerebral infarction. *J Thorac Cardiovasc Surg* 128: 378-385, 2004.

2. Ibaraki K, Yamamoto S, Fan W, Terakawa S. Acute DNA fragmentation detected by comet assay in excitotoxicity. *Neurotrauma Res* 16: 36-38, 2004

3. Sakurai T, Wakazono Y, Yamamoto S, Terakawa S: Slit-scanning microscope with a high NA objective lens for analysis of synaptic function. *Proc SPIE* 5322: 108-113, 2004

4. Koide M, Nishizawa S, Yamamoto S, Yamaguchi M, Namba H, Terakawa S: Nicotine exposure, mimicked smoking, directly and indirectly enhanced protein kinase C activity in isolated canine basilar artery, resulting in enhancement of arterial contraction. *J Cereb Blood Flow Metab,* 25: 292-301, 2005.

5. Ibaraki K, Yamamoto S, Wang Y, Terakawa S. Morphological changes of hippocampal neurons in AMPA (alpha-amino-3-hydroxy-5-methyl-4-isoxazole propionic acid)-mediated excitotoxicity. *Neurotrauma Res*. 17:36-38, 2005

6. Wang Y, Yamamoto S, Ibaraki K, Miyakawa A, Sakurai T, Terakawa S. Free radical production in rat ischemic brain measured by intravital fluorescence imaging. *Neurotrauma Res*. 17:24-28, 2005

7. Osawa S, Kajimura M, Yamamoto S, Ikuma M, Mochizuki C, Iwasaki H, Hishida A, Terakawa S. Alteration of intracellular histamine H2 receptor cycling precedes antagonist-induced up-regulation. *Am J Physiol, Gastrointest Liver Physiol* 289: G880-G889, 2005

8. Yamamoto J, Hirano T, Li S, Koide M, Kohno E, Inenaga C, Tokuyama T, Yokota N, Yamamoto S, Terakawa S, Namba H. Selective accumulation and strong photodynamic effects of a new photosensitizer, ATX-S10 · Na (II), in experimental malignant glioma. *Int J Oncol* 27: 1207-1213, 2005

9. Aoyagi K, Sugaya T, Umeda M, Yamamoto S, Terakawa S, Takahashi M. The activation of exocytotic sites by the formation of phosphatidylinositol 4,5-bisphosphate microdomains at syntaxin clusters. *J Biol Chem* 280: 17346-17352, 2005

10. Ibaraki K, Yamamoto S, Fan W, Terakawa S. Comet assay revealed that DNA fragmentation rapidly occurred in neuronal necrosis. Program No. 96.23. 2005 *Abstract Viewer/Itinerary Planner. Washington, DC: Society for Neuroscience, 2005.* Online, 2005

11. Sakurai T, Yamamoto S, Miyakawa A, Wakazono Y, Yoshida TO, Kohno E, Tsuchiya-Suzuki R, Wang Y, Hirukawa H, Terakawa S. Fiber-coupled confocal microscope (FCM) for real time imaging of cellular signals in vivo. *Proc SPIE* 6088:608803-1 - 608803-5, 2006

12. Wakazono Y, Sakurai T, Ohara-Imaizumi S, Nagamatsu S, Yamamoto S, Terakawa S. Intracellular dynamics observed by mode switching of microscope with a light incidence to the interface at alternate angles through the ultra high NA objective. *Proc SPIE* 6088:60881L-1 - 60881L-6, 2006

13. Yamamoto S, Wang Y, Ibaraki K, Sakurai T, Terakawa S. Intravital fluorescence imaging revealed that intracellular calcium ion persistently increases following transient forebrain ischemia in rat hippocampus. Program No. 588.1. 2005 *Abstract Viewer/Itinerary Planner. Washington, DC: Society for Neuroscience, 2005*. Online, 2005

14. Yamamoto S, Ibaraki K, Tsuboi T, Sakurai T, Terakawa S: Further evidence for the role of inositol trisphosphate as an excitotoxic death signal in hippocampal neurons. http://www.nature.com/jcbfm/journal/v25/n1s/full/9591524.0446.html. online, *J Cereb Blood Flow Metab* 25, S446, 2005

15. Yoshida TO, Kohno E, Sakurai T, Hirano T, Yamamoto S, Terakawa S. Model for monitoring the process of photodynamic therapy in patients. *Proc SPIE* 5967: 182-186, 2005

16. Tsagaan B, Abe K, Goto M, Yamamoto S, Terakawa S. Segmentation of brain volume based on 3-D region growing by integrating intensity and edge for image-guided surgery. *Proc SPIE* 6141:61412D-1 - 61412D-8, 2006

17. Tsagaan B, Abe K, Iwai K, Yamamoto S, Terakawa S. Registration of laser range image of cortical surface to preoperative brain MR images for image-guided neurosurgery: preliminary results. *Proc SPIE* 6141:61412C-1 – 61412C-7, 2006

18. Namba H, Tokuyama T, Yokota N, Sakai N, Tanaka T, Yamamoto S, Terakawa S, Tsagaan B, Abe K: Image-Guided Surgery for Gliomas. *Minimally Invasive Neurosurgery and Multidisciplinary Neurotraumatology*. Eds. T. Kanno and Y. Kato. Springer-Verlag Tokyo 2006. pp22-28, 2006

19. Yamamoto J, Yamamoto S, Hirano T, Li S, Koide M, Kohno E, Okada M, Inenaga C, Tokuyama T, Yokota N, Terakawa S, Namba H. Monitoring of singlet oxygen is useful for predicting the photodynamic effects in the treatment for experimental

glioma. *Clinical Cancer Res*, 12(23):7132-7139, 2006

20. Tsagaan B, Iwami K, Abe K, Nakatani H, Yamamoto S, Terakawa S. Newly developed navigation system for paranasal sinus surgery. *Int J CARS (Computer Assisted Radiology and Surgery)* 1: 502-503, 2006

21. Suzuki T, Kazui T, Yamamoto S, Washiyama N, Ohkura K, Ohishi K, Bashar AH, Yamashita K, Terada H, Suzuki K, Akuzawa S, Fujie M . Effect of prophylactically administered edaravone during antegrade cerebral perfusion in a canine model of old cerebral infarction. *J Thorac Cardiovasc Surg* 133:710-716, 2007

22. Yamamoto S, Yamada J, Ueno S, Kubota H, Furukawa T, Yamamoto S, Fukuda A. Insertion of α7 nicotinic receptors at neocortical layer V GABAergic synapses is induced by a benzodiazepine, midazolam. *Cereb Cortex*, 17:653-660, 2007

1-B) 邦文

1．山本清二，櫻井孝司，若園佳彦，寺川　進　ビデオイメージングによる生細胞機能解析．　医学のあゆみ　210，172-176，2004

2．山本清二，櫻井孝司，若園佳彦，寺川　進：ビデオイメージングによる生細胞機能解析．医学のあゆみ　210：1172-1176，2004

3．小出昌代、西澤茂、山本清二、難波宏樹、寺川 進：喫煙を模したnicotineの低濃度長期暴露が脳血管トーヌスの調節に与える影響について．脳卒中の外科（増刊号）32（脳血管攣縮20），68-73，2004

(2) 学会発表

2-A) 国際学会

1. Yamamoto S, Golanov EV: Stabilizing effect of cerebellar fastigial nucleus stimulation on neuronal mitochondrial membrane potential. Experimental Biology (FASEB), 2004. 4. 17-21, Washington DC, USA

2. Golanov EV, Yamamoto S: Uncoupling Protein 4: possible involvement in neurogenic neuroprotection. Experimental Biology (FASEB), 2004. 4. 17-21, Washington DC, USA

3. Yamamoto S, Tsuboi T, Sakurai T, Wakazono Y, Terakawa S: Inositol trisphosphate pathway as a death signal induced by mitochondrial toxin in the hippocampal neurons. Society for Neuroscience 34th Annual Meeting, 2004. 10. 23-27, San Diego, Ca, USA.

4. Yamamoto S, Wang Y, Ibaraki K, Sakurai T, Terakawa S: Intravital fluorescence imaging revealed that intracellular calcium ion persistently increases following transient forebrain ischemia in rat hippocampus. Society for Neuroscience 35th Annual Meeting, 2005. Nov 12-16, Washington DC, USA

5. Ibaraki K, Yamamoto S, Fan W, Terakawa S. Comet assay revealed that DNA fragmentation rapidly occurred in neuronal necrosis. Society for Neuroscience 35th Annual Meeting, 2005. 11. 12-16, Washington DC, USA

6. Yamamoto S, Ibaraki K, Tsuboi T, Sakurai T, Terakawa S: Further evidences for the role of inositol trisphophate as an excitotoxic death signal in hippocampal neurons. 22nd International Symposium on Cerebral Blood Flow, Metabolism, and Function & 7th International Conference on Quantification on Brain Function with PET

(Brain '05 & BrainPET '05), 2005. 6. 7-11, Amsterdam, Netherlands

7. Sakurai T, Yamamoto S, Miyakawa A, Wakazono Y, Terakawa S. Fiber-coupled confocal microscope (FCM) for real time imaging of cellular signals in vivo. Photonics West, 2006. 1.21-26, SanJose, USA

8. Yamamoto S, Wang Y, Ibaraki K, Sakurai S, Terakawa S. Transient forebrain ischemia induces long lasting increase in intracellular calcium ion in CA1 but not in CA3 in rat hippocampus. Neuroscience 2006, the Society's 36th Annual Meeting. 2006. 10.14-18, Atlanta, USA

9. Tsagaan B, Iwami K, Abe K, Nakatani H, Yamamoto S, Terakawa S. Newly developed navigation system for paranasal sinus surgery, CARS 2006, Computer Assisted Radiology and Surgery, 20th International Congress Meeting. 2006.6.28-7.1, Osaka, Japan

2-B) 国内学会

1．山本清二：光によるイメージングの現状と将来（特別講演）．第17回バイオメディカル分析化学シンポジウム，2004. 6. 4-6　西宮

2．山本清二：浜松医科大学光量子医学研究センターと医工・産学連携（特別講演）．浜松商工会議所定例技術交換研究会，2005. 3. 30　浜松

3．山本清二、范　文英、櫻井孝司、若園佳彦、坪井貴司、寺川　進：ミトコンドリア障害によるイノシトール三リン酸を介した神経細胞核DNAの急性断片化．第81回日本生理学会大会，2004．6．2-4，札幌.

4．范　文英、山本清二、若園佳彦、櫻井孝司、寺川　進：培養海馬神経細胞におけるグルタミン酸によるカスパーゼ３の活性化．第81回日本生理学会大会，2004．6．2-4，札幌．

5．山本清二、范　文英、櫻井孝司、若園佳彦、寺川　進：急性および遅発性神経細胞死においてグルタミン酸により活性化されるカスパーゼ：第27回日本神経科学大会・第47回日本神経化学大会合同大会．2004.9.21-23，大阪

6．山本清二、山本淳考、平野　達、寺川　進、難波宏樹：光線力学療法に用いる新規光増感剤ATX-S10Na(II)による脳腫瘍イメージング．第63回日本脳神経外科学会総会，2004．10．6-8，名古屋

7．山本淳考、平野　達、山本清二、難波宏樹：新しい光感受性薬剤ATX-S10Na(II)を用いた悪性脳腫瘍に対する蛍光診断および光線力学両方療法．第63回日本脳神経外科学会総会，2004．10．6-8，名古屋

8．茨木京子、山本清二、若園佳彦、櫻井孝司、寺川　進：興奮性神経細胞死における急性DNA断片化のコメットアッセイによる検出．第16回神経損傷の基礎シンポジウム．2004．11．20，東京

9．山本淳考、平野　達、河野栄治、李　少一、小出昌代、徳山　勤、横田尚樹、山本清二、寺川　進、難波宏樹：悪性脳腫瘍に対する光線力学療法 －近赤外微弱光検出による一重項酸素のモニタリングー．第1回日本脳神経外科光線力学研究会．2005.2.12，東京

１０．山本清二：イメージングによる神経細胞死のメカニズムの解析 －１分子から個体レベルまでー（特別講演）．第8回岡山スリースライドカンファレ

ンス，2005.5.11　岡山市、岡山

１１．山本清二：集中治療における光テクノロジーの応用（特別講演）．第13回日本集中治療医学会東海北陸地方会，2005.6.18　浜松市、静岡

１２．茨木京子、山本清二、寺川　進：AMPA受容体依存性興奮性神経毒性における海馬神経細胞の形態変化．第17回神経損傷の基礎シンポジウム．2005.12.3．東京

１３．王　勇、山本清二、宮川厚夫、櫻井孝司、寺川　進：生体内蛍光イメージングによるラット脳虚血時のフリーラジカル産生の評価．第17回神経損傷の基礎シンポジウム．2005.12.3．東京

１４．櫻井孝司、山本清二、宮川厚夫、若園佳彦、秋山　喬、寺川　進：ファイバー式共焦点顕微鏡（FMC）によるin situ リアルタイム細胞イメージング．第82回日本生理学会大会．2005.5.18-20．仙台

１５．若園佳彦、櫻井孝司、宮川厚夫、山本清二、寺川　進．Digital Micromirror Device（DMD）を照明系に用いた新たな顕微鏡システムの開発．第82回日本生理学会大会．2005.5.18-20．仙台

１６．山本純偉、山田順子、上野伸哉、窪田寿彦、山本清二、福田敦夫：ベンゾジアゼピンによる大脳皮質第Ｖ層のGABA作動性シナプスにおけるα７ニコチン受容体のinsertionはPKCを介する．第82回日本生理学会大会．2005.5.18-20．仙台

１７．山本清二、Golanov EV：小脳室頂核電気刺激による神経細胞ミトコンドリア機能の強化．第82回日本生理学会大会．2005.5.18-20．仙台

１８．茨木京子、山本清二、范　文英、寺川　進：コメットアッセイにより検出された興奮性神経細胞死における急性DNA断片化．第82回日本生理学会大会．2005.5.18-20．仙台

１９．茨木京子、山本清二、范　文英、寺川　進：ネクロー シス型神経細胞死における急性DNA断片化のコメットアッセイによる解析．第28回日本神経科学大会．2005.7.26-28．横浜

２０．山本清二、茨木京子、坪井貴司、櫻井孝司、寺川　進：急性興奮性神経細胞死のDNA断片化に重要な役割を果たすイノシトール三燐酸による核カルシウムシグナル．第28回日本神経科学大会．2005.7.26-28．横浜

２１．山本清二、王　勇、櫻井孝司、寺川　進：生体内蛍光イメージングによるラット脳虚血モデルでのカルシウム反応．第64回日本脳神経外科学会総会．2005.10.5-7．横浜

２２．山本淳考、山本清二、河野栄治、小出昌代、徳山　勤、横田尚樹、寺川進、平野　達、難波宏樹：悪性グリオーマにおける、Photodynamic therapyにより発生する一重項酸素と細胞死の関係．第64回日本脳神経外科学会総会．2005.10.5-7．横浜

２３．山本清二、王　勇、櫻井孝司、寺川　進：ラット一過性前脳虚血における 海馬*in situ* カルシウム反応．第17回日本脳循環代謝学会総会．2005.11.25-26．名古屋

２４．山本淳考、谷　春雨、岡田満夫、稲永親憲、徳山　勤、横田尚樹、難波宏樹、平野　達、河野栄治、山本清二、寺川　進．Photodynamic therapy

(PDT) により誘発される細胞死と発生する一重項酸素との関係 —in vivo study—. 第2回日本脳神経外科光線力学研究会. 2006.2.4. 神戸

２５．吉田孝人、河野栄治、桜井孝司、山本清二、平野　達、寺川　進：治療過程をモニタリングする新しい光線力学的治療システムの開発。第１５回日本光線力学学会プログラム・抄録集、19頁、6月11日2005、磐田。

２６．若園佳彦、櫻井孝司、宮川厚夫、山本清二、寺川　進. ガルバノミラーを用いた全反射および落射照明の高速切替システムによるPKCαの細胞膜移行の観察. 第14回日本バイオイメージング学会学術集会. 2005.10.26-28. 東京

２７．山本清二：イメージングによる脳蘇生・神経細胞死の病態解析（特別講演）. 日本蘇生学会第２５回大会, 2006.12.1-1 浜松

２８．山本清二、渡邉高弘、細川誠二、竹下　有、峯田周幸、バイガルマ・ツァガーン、阿部圭一、中谷広正、寺川　進. 新しい副鼻腔手術用光学式ナビゲーションの開発. 新しい副鼻腔手術用光学式ナビゲーションの開発（指定演題）第２２回静岡県耳鼻咽喉科手術手技研究会. 2007.3.10. 静岡

２９．山本清二：光でからだを診て、治す！？（シンポジウム）　日本比較生理生化学学会第２８回大会・一般公開シンポジウム. 2006.7.29 浜松

３０．山本清二、寺川　進：神経細胞死の信号をイメージングで解析する（シンポジウム）. ２１世紀COEプログラムジョイントシンポジウム「知の創造と知の集積－静岡からの発信」2006.3.15, 静岡

３１．山本清二、渡邉高弘、岩崎　聡、細川誠二、竹下　有、峯田周幸、バイ

ガルマ・ツァガーン、阿部圭一、中谷広正、寺川　進．新しい副鼻腔手術用光学式ナビゲーションの開発．第8回耳鼻咽喉科手術ナビゲーション（手術支援システム）研究会．2006.10.14 松本

３２．山本清二、王　勇、茨木京子、櫻井孝司、宮川厚夫、寺川　進：生体内カルシウムイメージングにより観察したラット一過性前脳虚血後の脳内カルシウム反応は海馬CA1領域と大脳皮質で異なる．第29回日本神経科学大会．2006.7.19-21，京都

３３．山本清二、王　勇、櫻井孝司、寺川　進：ラット一過性前脳虚血による in situカルシウム反応からみた海馬CA1領域とCA3領域の差異．第１８回日本脳循環代謝学会総会．2006.11.10-11 東京

３４．茨木京子、山本清二、王勇、寺川進：AMPA induced excitotoxic morphological changes in hippocampal neurons.第49回 日本神経化学会大会、第28回 日本生物学的精神医学会、第36回 日本神経精神薬理学会 3学会合同年会．2006.9.14-16 名古屋

３５．茨木京子、山本清二、宮川厚夫、寺川進：AMPA受容体依存性興奮性神経毒性における海馬神経細胞死の解析．第18回神経損傷の基礎シンポジウム．2006.12.2 東京

Intravital cell imaging of the cerebral cortex upon ischemia-reperfusion in rats

Summary

In this study, we established a new semi-quantitative analysis system that can spatiotemporally detect the cortical intracellular production of reactive oxygen species (ROS). Ischemia/reperfusion-dependent production of superoxide radical ($\cdot O_2^-$) and hydroxyl radical ($\cdot OH$) were measured by intravital imaging. Transient (10min) forebrain ischemia (4-vessel occlusion) followed by 20-minute reperfusion was induced by coagulating bilateral vertebral arteries and occluding bilateral common carotid arteries with balloon occluders. Then the fluorescence changes of MitoSOX (a fluorescent indicator for mitochondrial $\cdot O_2^-$ generation) or hydroxyphenyl fluorescein (HPF, a fluorescent indicator for $\cdot OH$ production) in the cortex were measured under a confocal microscope. In the present study, the intravital imaging indicated that $\cdot O_2^-$ and $\cdot OH$ production increased in the early period of reperfusion but not during the ischemia. Especially, during reperfusion, production of $\cdot OH$, toxic reactive oxygen species, was more dominant than $\cdot O_2^-$.

***Key words*:**

forebrain ischemia, reactive oxygen species, intravital imaging, cerebral cortex

Introduction

Free radicals contribute to the cell damage in brain ischemia (Cross CE et al., 1987). Cerebral ischemia and reperfusion enhance production of reactive oxygen species (ROS), which can cause membrane damage or enzyme inactivation due to lipid peroxidation and/or protein oxidation (Floyd RA and Carney JM, 1992; Halliwell B, 1992), resulting in disruption of cellular homeostasis. Thus sensitive, specific, and reliable methods to detect changes in ROS are essential to understand the roles of these substances in the both normal and diseased states.

Several studies using electron-spin resonance showed increased oxygen free radical formation during ischemia (Zini I et al., 1992; Phillis JW and Sen S 1993; Piantadosi CA and Zhang J, 1996). However, the results remain controversial. Oliver CN et al. showed no evidence of increased free radicals at the end of 10-min ischemia in gerbil (Oliver CN et al., 1990). In the present study, to analyze the controversial issue, we tried to establish a new semi-quantitative analysis system that could spatiotemporally detect the cortical intracellular oxygen radical changes of adult rat brain, and sought to determine how the production of oxygen radicals could change in ischemia-reperfusion.

Methods

Adult male Sprague-Dawley rats (300 g, SLC Inc., Japan) were anesthetized and spontaneously ventilated. After instrumentation, bilateral vertebral arteries were coagulated, and transient (10 min) forebrain ischemia was induced by occluding bilateral common carotid arteries with balloon occluders (Unique Medical Inc. Tokyo, Japan). The regional cerebral blood flow (rCBF) was measured by laser-Doppler flowmetry.

To observe the oxygen radical production, cranial window (3×3mm、center at 3.6 mm caudal and 2 mm lateral to the Bregma) was made over the frontal cortex, and a

fluorescent dye (2.5 μl) was microinjected (by pressurized bolus injection) into the cortical region. MitoSOX (5μM, Ex/Em=510/580nm, Molecular probes, Invitrogen, USA), a fluorescent dye for mitochondrial superoxide radical ($\cdot O_2^-$) production, was used. To measure hydroxyl radical (·OH) production, hydroxyphenyl fluorescein (HPF) (20 μM, Ex/Em=490/515nm, Daiichi Pure Chemicals, Japan), a fluorescent ·OH indicator, was used. After microinjection, closed cranial window was made over the cortex, and the fluorescence images were taken under a microscope (BX50WI, Olympus, Japan) equipped with a confocal scanner of a microlens-attached Nipkow-disk (CSU-21, Yokogawa, Japan) every 30 s before and after 10-min ischemia.

Results

1. rCBF change during ischemia and reperfusion in the cortex

Mean arterial pressure and blood gases were within normal limits for anesthetized rats, and did not differ among the groups. During 10-min ischemia, the rCBF (mean ± SD, n=6) dropped to 29 ± 7 %, and returned to the baseline level with a slight hyperemia after reperfusion (**Fig 1**).

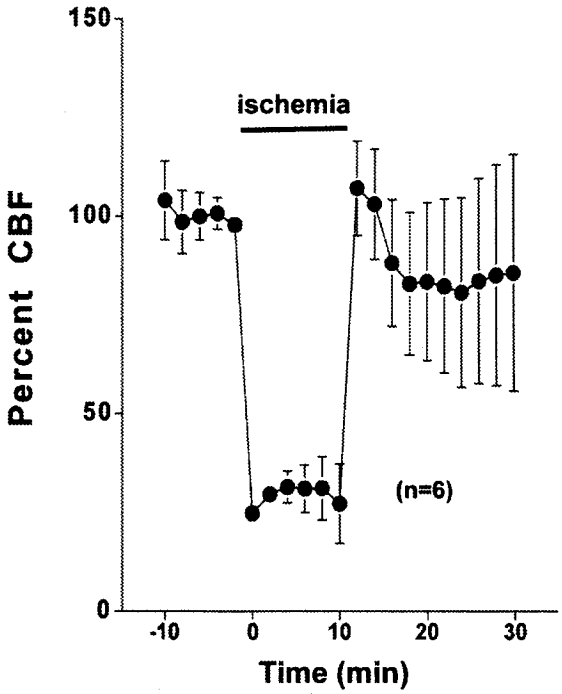

Fig. 1 rCBF change following 4-vessel occlusion
The rCBF of cortex (mean ± SD, n=6) was approximately 29 ± 7 % of baseline during 4-vessel occlusion. At the onset of reperfusion, the rCBF returned to the base-line in 6 minutes with a hyperemic peak.

2. Changes in the fluorescence intensity of MitoSOX and HPF in the cortex

In the control animals without ischemia, $\cdot O_2^-$ and ·OH did not significantly increase (n=3/each). During 10-min ischemia, the

fluorescence intensity of MitoSOX (n=5) began to significantly increase at the 5 min after the onset of ischemia, reached to 160±13% at the end of ischemia, and persistently increased up to 186±20% during 20-min reperfusion (**Fig 2 and 3**). The ·fluorescence intensity of HPF (n=5) started to increase at the 5 min after the onset of ischemia, elevated to 131±12% at the end of ischemia, and persistently increased up to 183±10% during reperfusion (**Fig. 2**).

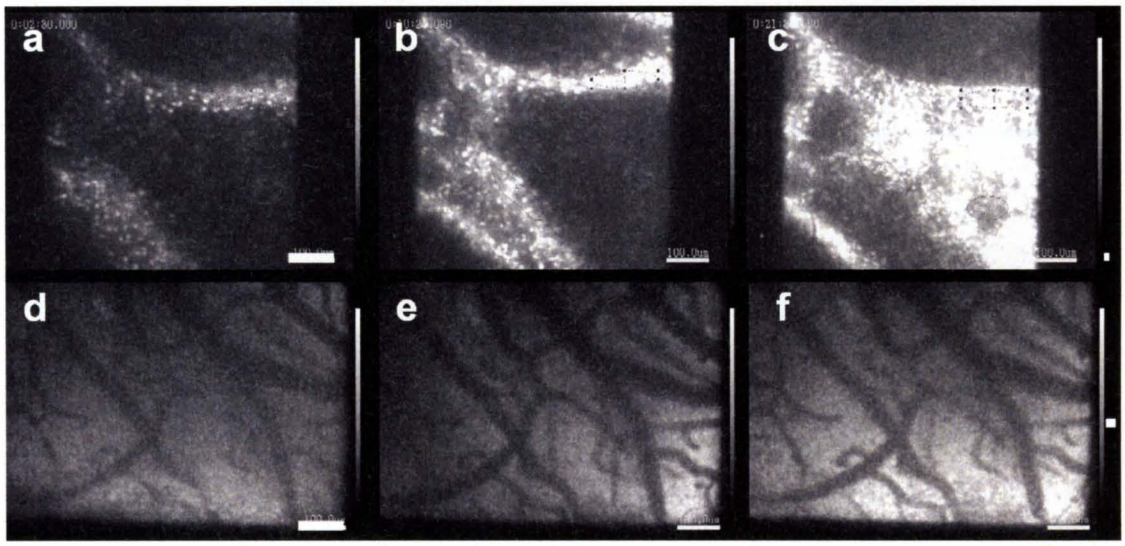

Fig. 2 Representative fluorescence images of MitoSox (a-c) and HPF (d-f)
Images were taken before ischemia (a, d), 10 min after ischemia (b, e), and 10 min after reperfusion (c, f). Scale bar = 100 μm.

3. Effect of ischemia-reperfusion on the fluorescence in the cortex

Since the hemoglobin absorbs both excitation and emission light, ischemia may affect the fluorescent intensity of dye inside the brain. To analyze the effects of ischemia on the fluorescence intensity, the fluorescent microspheres (0.2 μm diameter, similar excitation and emission to those of dye) were microinjected with pulse pressure into the cortex and the images were taken before and after 10-min ischemia in the same manner as did in the MitoSOX and HPF imaging.

The fluorescence of microspheres (510/560nm, and 490/515nm, n=3/each) microinjected in the cortex increased to 130±13.7% of base line during ischemia and returned to the baseline immediately after reperfusion (**Fig. 4**). In the fluorescence imaging, therefore, the data during ischemia was corrected based on the results studied using microfluospheres.

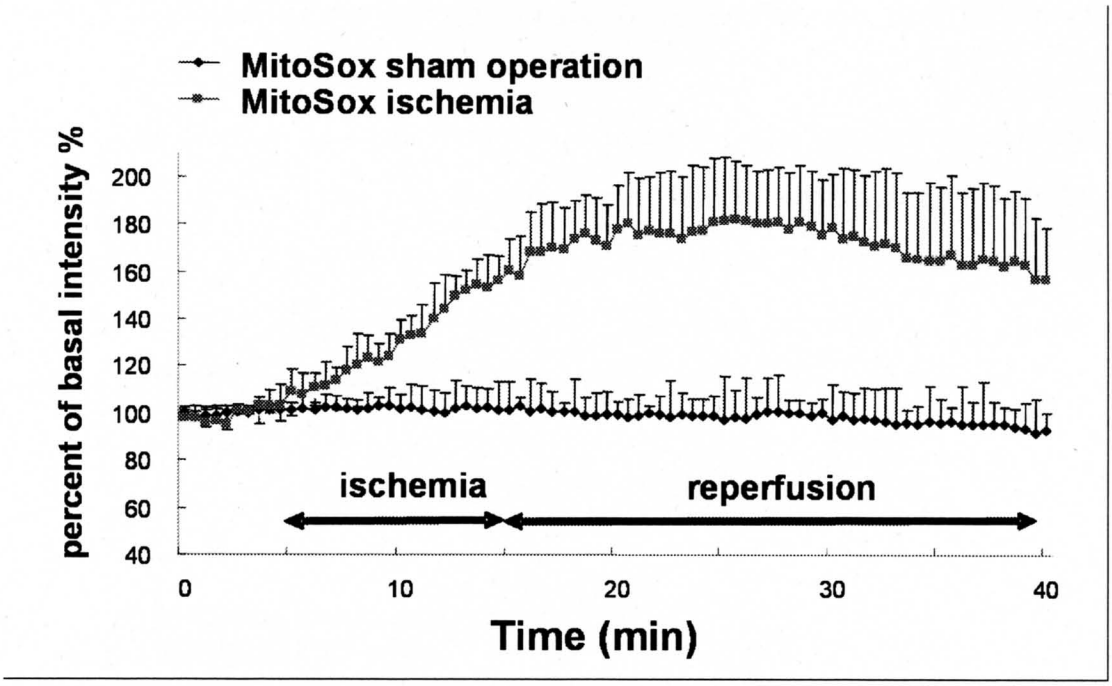

Fig. 3 Raw data of the changes in fluorescence intensity of MitoSox upon ischemia-reperfusion

The change in fluorescence of MitoSox in the cortex was measured.with (■:ischemia) or without (◆:sham operation) ischemia. Note that the fluorescence increased in the ischemia group.

n = 3/each, values are mean ± SD

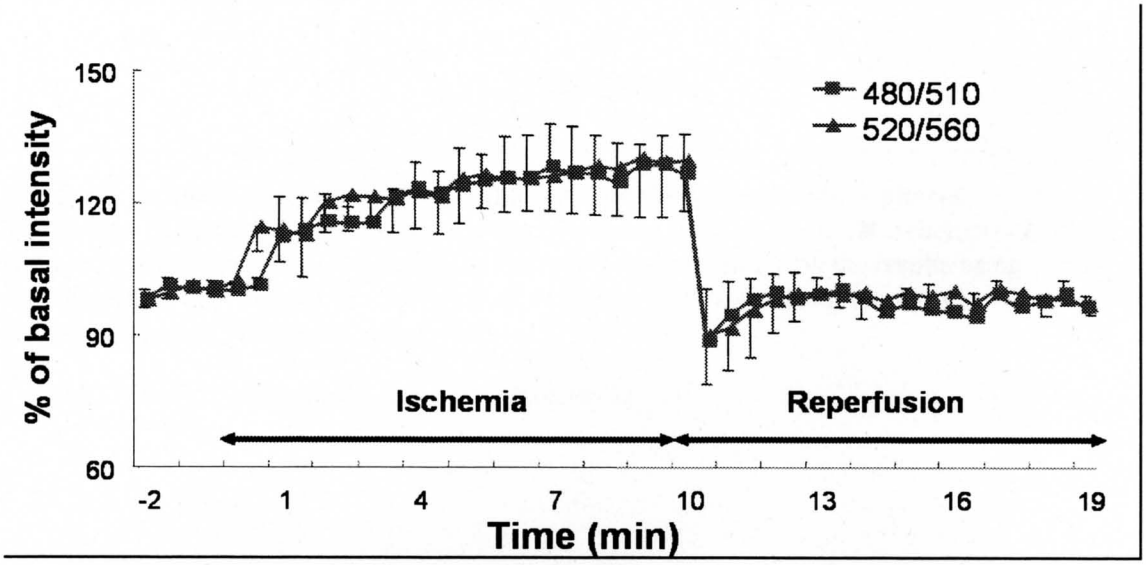

Fig. 4 Changes in fluorescence upon ischemia-reperfusion

The change in fluorescence of microfluospheres in the cortex was measured. Note that the fluorescence increased up to 130% in ischemia and return to baseline in reperfusion.

■:Ex/Em = 480/510 nm (similar to HPF)

▲:Ex/Em = 520/560 nm (similar to MitoSox)

n = 5, values are mean ± SD

4. Corrected data showed the increase in fluorescence intensity only in reperfusion period

In the MitoSOX group, a transient forebrain ischemia led to a low increase of MitoSOX fluorescence (up to 125±11%); but during reperfusion, it increased significantly up to 179±18% (**Fig 5**). In the HPF group, no increase in the fluorescence intensity was observed during 10-min ischemia. However following reperfusion, it significantly increased to 187±10% over the baseline (**Fig 6**).

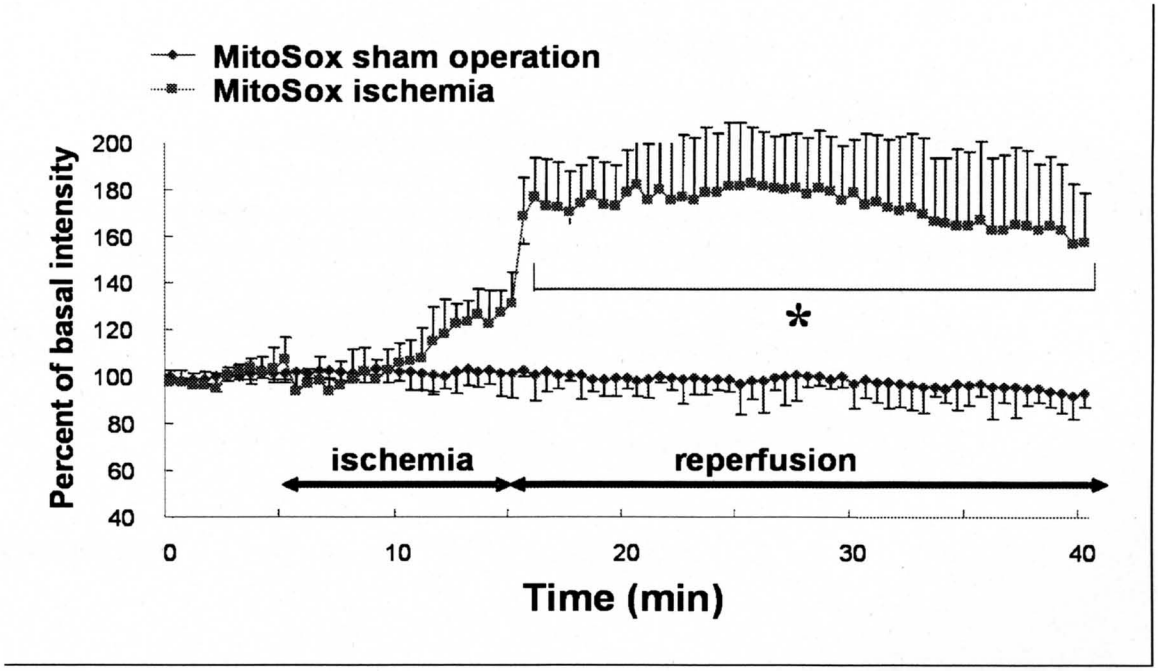

Fig. 5 $\cdot O_2^-$ production corrected with the data obtained by microfluospheres
The change in fluorescence of MitoSox in the cortex was measured.with (■:ischemia) or without (◆:sham operation) ischemia, and the data were corrected with the results using microfluospheres. Note that the fluorescence increased in the ischemia group only in reperfusion period. Values are mean ± SD,

*
$p<0.01$ MitoSox ischemia vs. sham operation (n=5)

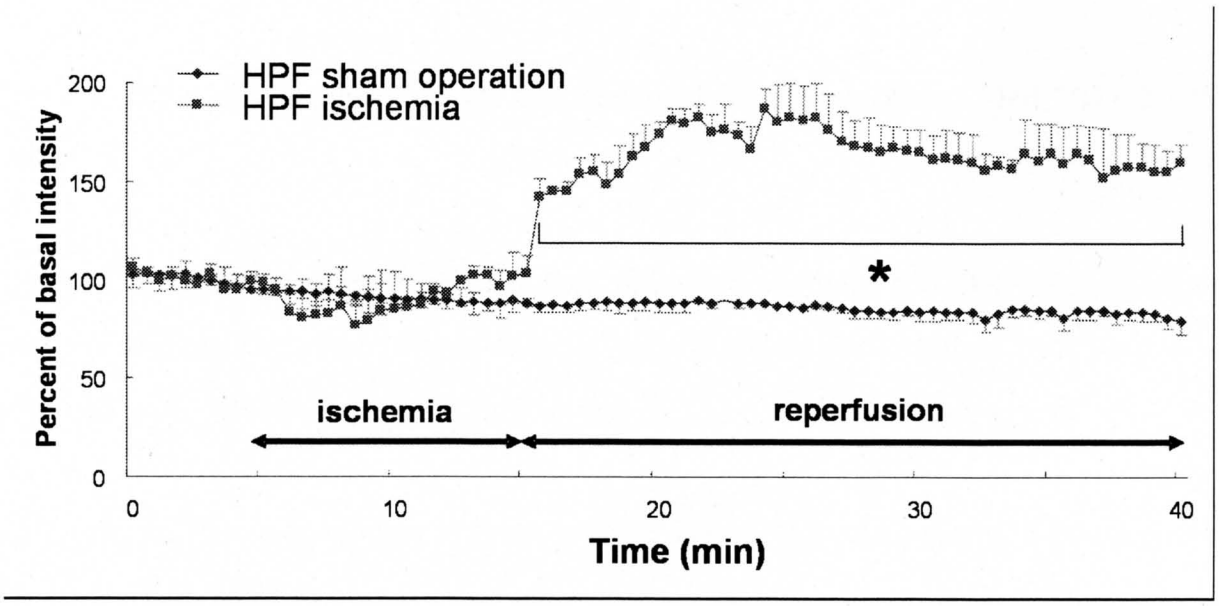

Fig. 6 ·OH production corrected with the data obtained by microfluospheres
The change in fluorescence of HPF in the cortex was measured.with (■:ischemia) or without (◆:sham operation) ischemia, and the data were corrected with the results using microfluospheres. Note that the fluorescence increased in the ischemia group only in reperfusion period. Values are mean ± SD,
*$p<0.01$ HPF ischemia vs. sham operation (n=5)

Comments

In the present study, the intravital imaging indicated that $\cdot O_2^-$ and ·OH production increased in the early period of reperfusion but not during the ischemia in rats. Especially, during the early period of reperfusion, production of ·OH, toxic reactive oxygen species, persistently increased, while $\cdot O_2^-$ did not do so. Our system allows us to observe real-time production of oxygen radicals, which is useful for investigating the pathological roles of free radical in the brain. Finally, we emphasize: 1) the effect of ischemia should be carefully analyzed in the study of intravital fluorescence imaging; and 2) our method using microsphere is useful.

References

Cross, C.E., et al., Oxygen radicals and human disease. Ann Intern Med 107:526-45, 1987

Floyd, R.A. and J.M. Carney, Free radical damage to protein and DNA: mechanisms involved and relevant observations on brain undergoing oxidative stress. Ann Neurol 32 Suppl:S22-27, 1992

Halliwell, B. Reactive oxygen species and the central nervous system. J Neurochem, 59: 1609-1623, 1992

Oliver, C.N., et al., Oxidative damage to brain proteins, loss of glutamine synthetase activity, and production of free radicals during ischemia/reperfusion-induced injury to gerbil brain. Proc Natl Acad Sci U S A, 87: 5144-5147, 1990

Phillis, J.W. and S. Sen, Oxypurinol attenuates hydroxyl radical production during ischemia/reperfusion injury of the rat cerebral cortex: an ESR study. Brain Res, 628:309-312.1993

Piantadosi, C.A. and J. Zhang, Mitochondrial generation of reactive oxygen species after brain ischemia in the rat. Stroke, 27:327-331, 1996

Zini, I., et al., Detection of free radicals during brain ischemia and reperfusion by spin trapping and microdialysis. Neurosci Lett, 138:279-282, 1992

Intravital cell imaging of the hippocampus in transient forebrain ischemia in rats

Summary

In the present study, we sought to determine, in rats, the $[Ca^{2+}]_i$ changes following transient forebrain ischemia in hippocampus. In anesthetized, spontaneously ventilated Sprague-Dawley rats (300 g), transient forebrain ischemia was induced. To obtain the intravital fluorescence image, we employed an imaging fiber bundle (1.0 mm outer diameter) including 20,000 fibers (4.5 μm outer diameter) coupled to the microlens-attached Nipkow-disk scanner (CSU-21, Yokogawa, Japan) equipped with 10x objective lens. This fiber-coupled confocal microscope (FCM) is capable to observe the confocal image just under the fibers. FCM was inserted stereotaxically into CA1 and CA3 regions, respectively. Fluo-3/AM (440 μM, 2.5 μl), a $[Ca^{2+}]_i$ sensitive fluorescent dye, was microinjected into the brain, and observed before and after ischemia with FCM. To analyze the effects of ischemia on the fluorescence intensity, the microfluospheres (0.2 μm diameter, similar excitation and emission to those of Fluo-3) were microinjected into hippocampus and the images were taken in the same manner as did in $[Ca^{2+}]_i$ imaging. Four-vessel occlusion decreased regional cerebral blood flow (rCBF) measured by laser-Doppler flowmetry, to 20-25%. They did not significantly differ in CA1 and CA3. 10-min forebrain ischemia significantly increased fluorescence intensity (mean ± SD %) of the microspheres in the hippocampus up to 108 ± 5 (n=4), which declined to the baseline level following reperfusion. In $[Ca^{2+}]_i$ imaging, therefore, the change in fluorescence during ischemia was corrected. During 10-min ischemia, the fluorescence intensity of Fluo-3 slightly increased up to 110 ± 9, and then increased to 134 ± 19 at the end of 20-min reperfusion in CA1 (n=4). In

contrast, in CA3 (n=5), the intensity did not change upon ischemia, and at reperfusion slightly elevated to 108 ± 4 without long-lasting increase. During 14-20 min reperfusion, the $[Ca^{2+}]_i$ increase in CA1 was statistically larger ($p < 0.05$) than that in CA3. In CA1, but not in CA3, transient forebrain ischemia induced long lasting Ca^{2+} increase *in situ*, whereas it produced similar rCBF changes in these regions. Since the $[Ca^{2+}]_i$ increase was significantly larger in CA1 during reperfusion period, it might reach to toxic levels and then mediate the vulnerability of CA1 against ischemia.

***Key words*:**

forebrain ischemia, calcium ion, intravital imaging, hippocampus

Introduction

In cultured neurons, the increase in intracellular Ca^{2+} concentration ($[Ca^{2+}]_i$) plays a crucial role in excitotoxicity (Yamamoto S et al., 2003; Matsumoto et al., 2004). However, in whole animals, calcium response following ischemia remains to be established. Especially, change in $[Ca^{2+}]_i$ in the hippocampus upon ischemia remains unclear, since no method has been available to measure the $[Ca^{2+}]_i$ in the deep structure of brain. In the present study, we sought to determine, in rats, the $[Ca^{2+}]_i$ changes following transient forebrain ischemia in hippocampus.

Methods

Adult male Sprague-Dawley rats (300 g, SLC Inc., Japan) were anesthetized and spontaneously ventilated. After instrumentation, bilateral vertebral arteries were coagulated, and transient (10 min) forebrain ischemia was induced by occluding bilateral common carotid arteries with balloon occluders (Unique Medical Inc. Tokyo, Japan). The regional cerebral blood flow (rCBF) was measured by laser-Doppler flowmetry.

To obtain the intravital fluorescence image, we employed an imaging fiber bundle (1.0 mm outer diameter) including 20,000 fibers (4.5 μm outer diameter) coupled to the microlens-attached Nipkow-disk scanner (CSU-21, Yokogawa, Japan) equipped with 10x objective lens. This fiber-coupled confocal microscope (FCM) is capable to observe the confocal image just under the fibers (Sakurai et al.). FCM was inserted stereotaxically into CA1 and CA3 regions, respectively. Fluo-3/AM (440 μM, 2.5 μl), a $[Ca^{2+}]_i$ sensitive fluorescent dye, was microinjected into the brain, and observed every 30 s before and after 10-min forebrain ischemia with FCM.

Since the hemoglobin absorbs both excitation and emission light, ischemia may affect the fluorescent intensity of Fluo-3 inside the brain. To analyze the effects of ischemia on the fluorescence intensity, the microfluospheres (0.2 μm diameter, similar

excitation and emission to those of Fluo-3) were microinjected into hippocampus and the images were taken before and after 10-min ischemia in the same manner as did in $[Ca^{2+}]_i$ imaging.

Results

1. rCBF change during ischemia and reperfusion in the hippocampus

Mean arterial pressure and blood gases were within normal limits for anesthetized rats, and did not differ among the groups. Four-vessel occlusion decreased CBF (mean ± SD %) measured by laser-Doppler flowmetry, to 25 ± 18 (n=6) in CA1 and to 20 ± 11 (n=6) in CA3 (**Fig 1**). They did not significantly differ.

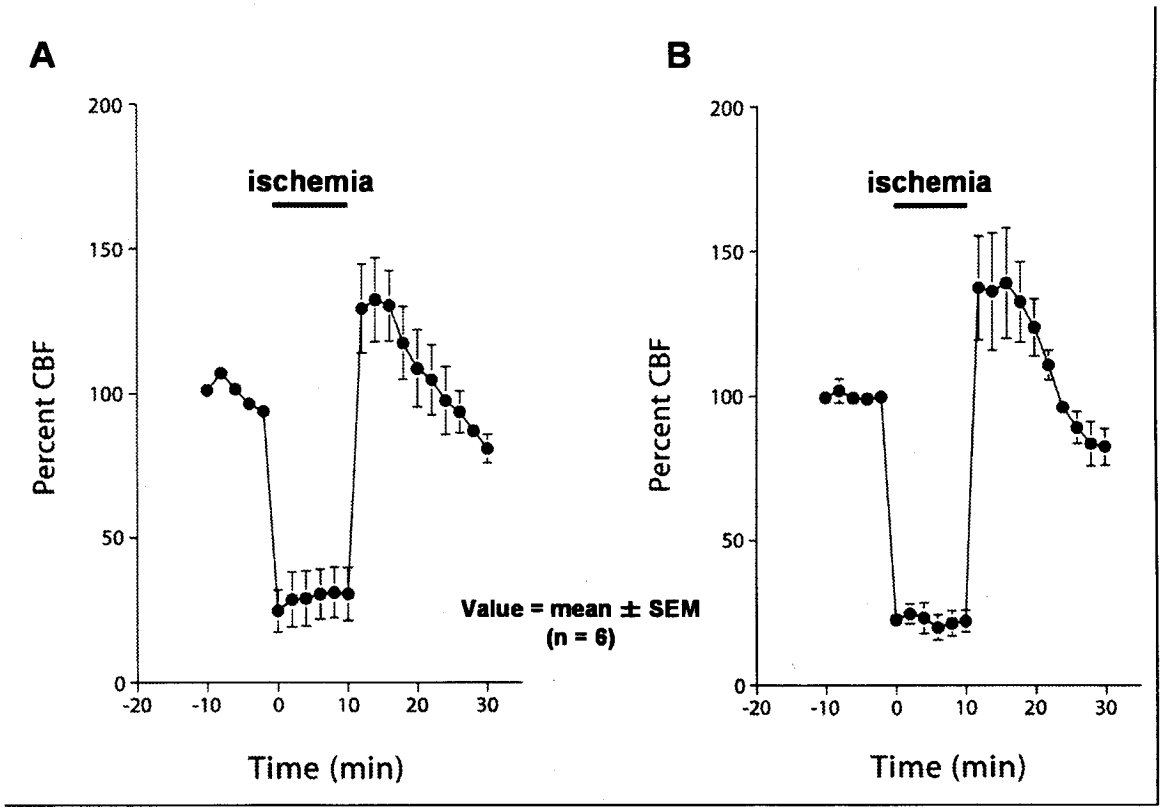

Fig. 1 rCBF change following 4-vessel occlusion in the hippocampus
The rCBF (mean ± SD, n=6) of the CA1 region (A) and CA3 region (B) were approximately 20 to 25 % of baseline during 4-vessel occlusion. At the onset of reperfusion, the rCBF returned to the base-line in 6 minutes with a hyperemic peak. There was no statistical difference between CA1 and CA3.

2. Effect of ischemia-reperfusion on the fluorescence in the hippocampus

To obtain the intravital fluorescence image, we employed the FCM, which is capable to observe the confocal image just under the fibers (**Fig. 2**) (Sakurai et al. 2006).

First of all, to analyze the effects of cerebral ischemia on the fluorescence inside the brain, microfluospheres (0.2 μm diameter, similar Ex and Em to those of Fluo-3) were observed using FCM. 10-min forebrain ischemia increased fluorescence intensity (mean ± SD %) of the spheres in the hippocampus up to 109% (n=6), which declined to the baseline level following reperfusion. In all measurements, the ischemia showed significant increase (**Fig 3**).

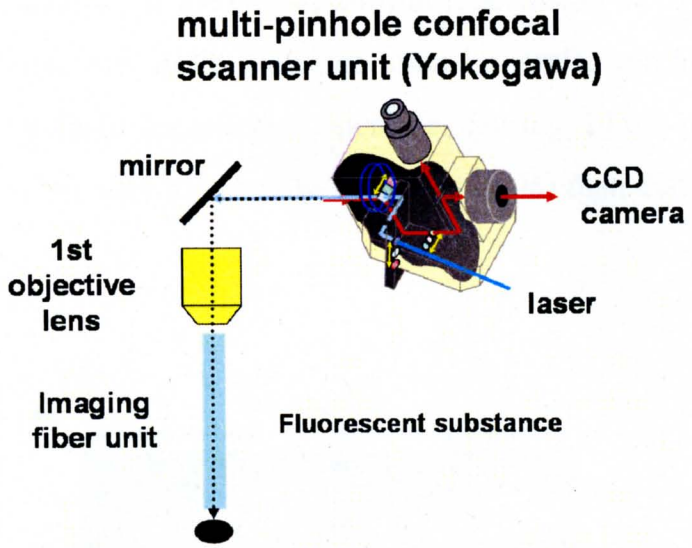

Fig. 2 Schematic presentation of fiber-coupled confocal microscope (FCM)

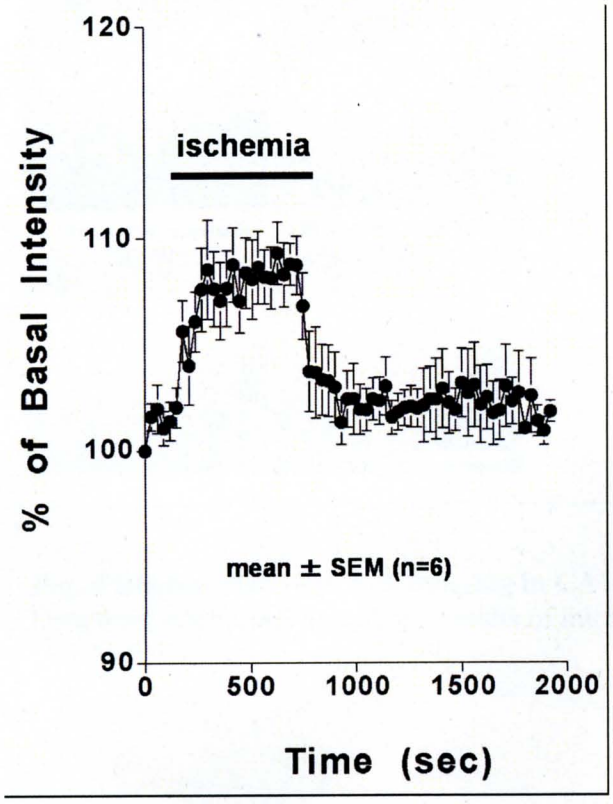

Fig. 3 Change in fluorescence intensity of microfluospheres upon ischemia.

Cerebral ischemia significantly increased fluorescence intensity up to 109 ± 1.5 %.

3. Changes in the fluorescence intensity of Fluo-3 in the hippocampus upon ischemia

In $[Ca^{2+}]_i$ imaging, therefore, the change in fluorescence during ischemia was corrected based on the results obtained with the microfluospheres. During 10-min ischemia, the fluorescence intensity of Fluo-3 slightly increased up to 110±9, and then increased to 134±19 at the end of 20-min reperfusion in CA1 (n=6). In contrast, in CA3 (n=5), the intensity did not change upon ischemia, and at reperfusion slightly elevated to 108±4 without long-lasting increase. During 14-20 min reperfusion, the $[Ca^{2+}]_i$ increase in CA1 was statistically larger ($p < 0.05$) than that in CA3 (**Fig. 4 and 5**).

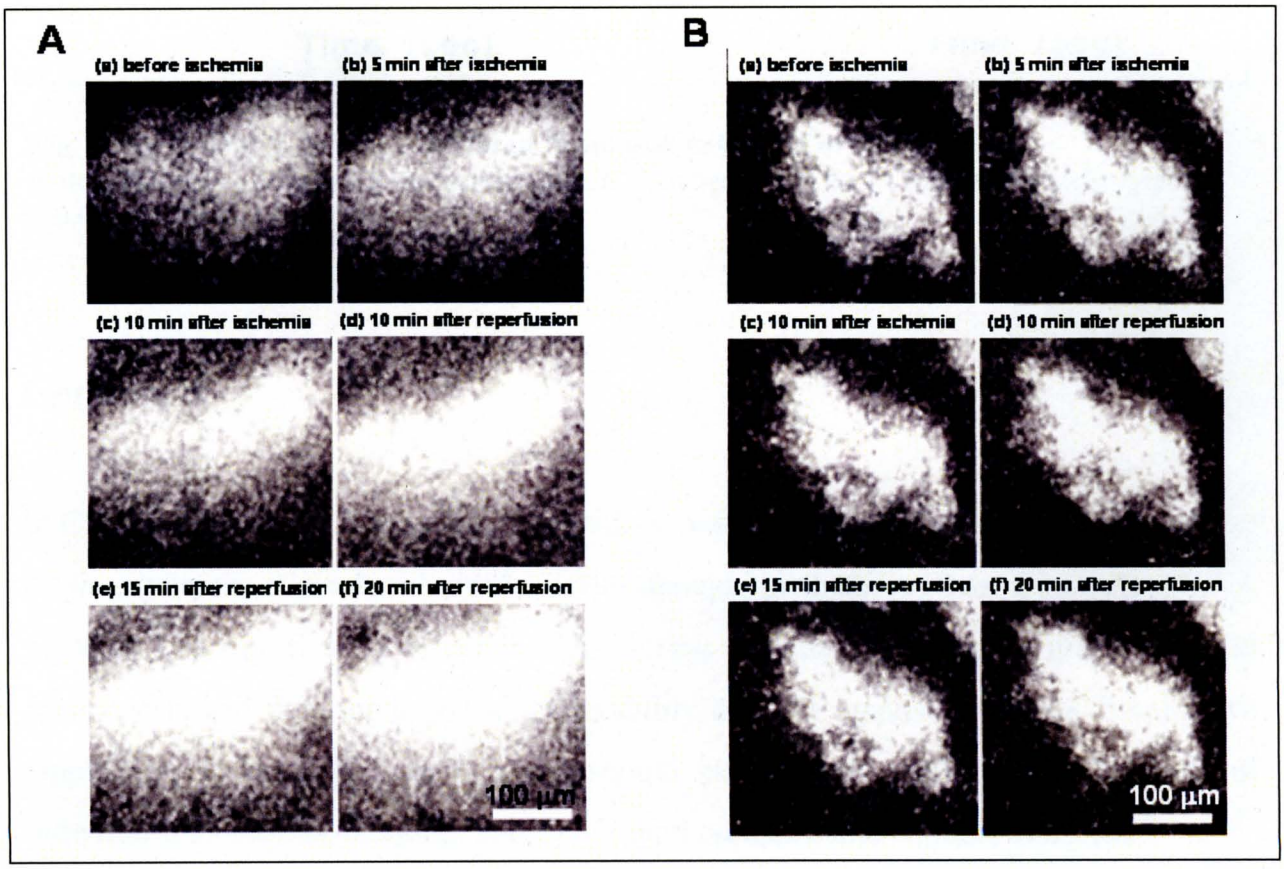

Fig. 4 Representative $[Ca^{2+}]_i$ imaging in CA1 (A) and in CA3 (B).
Data were not corrected with the results of microfluospheres. Bar = 100 μm.

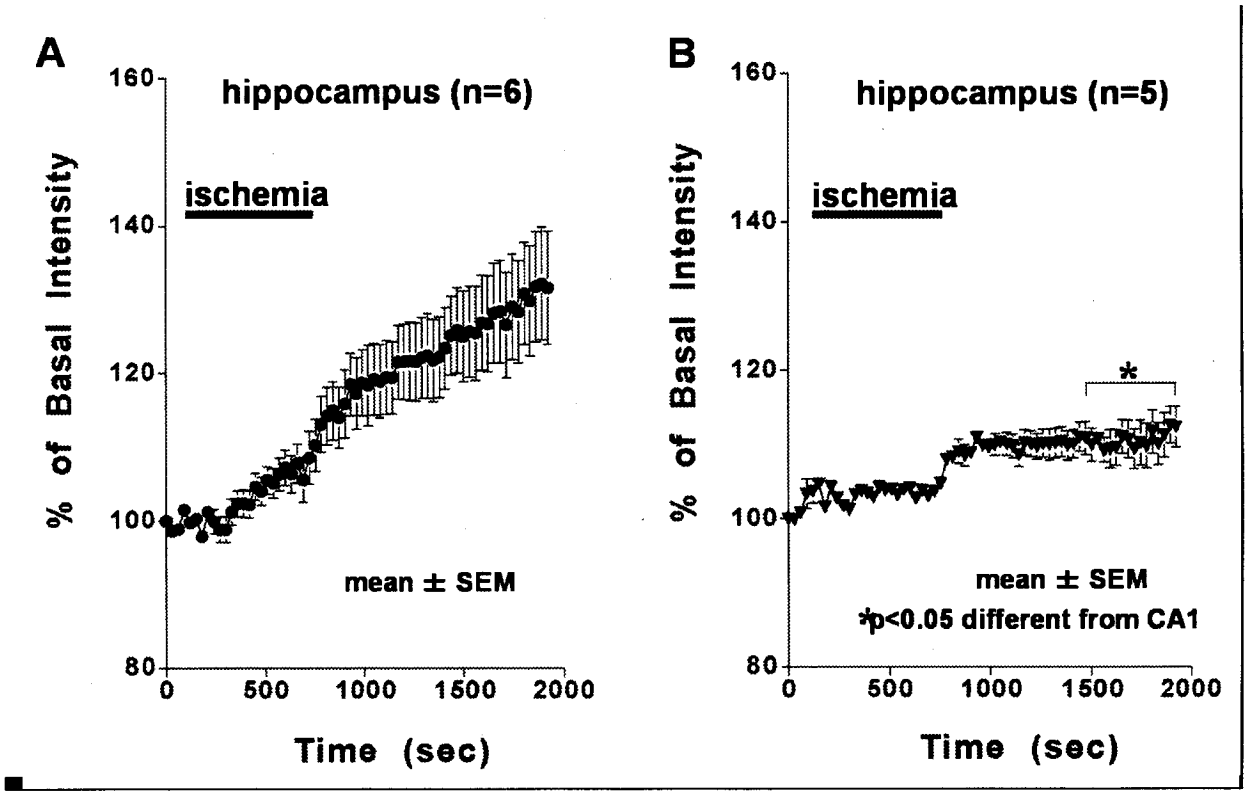

Fig. 5 $[Ca^{2+}]_i$ change in CA1 is different from that in CA3 (Corrected data).
Note that during 14-20 min reperfusion, the $[Ca^{2+}]_i$ increase in CA1 (A) was statistically larger ($p < 0.05$) than that in CA3 (B).

Comments

In CA1, but not in CA3, transient forebrain ischemia induced long lasting Ca^{2+} increase *in situ*, whereas it produced similar CBF changes in these regions. Since the $[Ca^{2+}]_i$ increase was significantly larger in CA1 during reperfusion period, it might reach to toxic levels and then mediate the vulnerability of CA1 against ischemia. Finally, we emphasize: 1) the effect of ischemia should be carefully analyzed in the study of intravital fluorescence imaging; and 2) our method using microsphere is useful.

References

Matsumoto Y, Yamamoto S, Suzuki Y, Tsuboi T, Terakawa S, Ohashi N, Umemura K: Na^+/H^+ exchanger inhibitor, SM-20220, is protective against excitotoxicity in cultured cortical neurons. Stroke 35: 185-190, 2004.

Sakurai T, Yamamoto S, Miyakawa A, Wakazono Y, Yoshida TO, Kohno E, Tsuchiya-Suzuki R, Wang Y, Hirukawa H, Terakawa S. Fiber-coupled confocal microscope (FCM) for real time imaging of cellular signals in vivo. Proc SPIE 6088:608803-1 - 608803-5, 2006

Yamamoto S, Matsumoto Y, Suzuki Y, Tsuboi T, Terakawa S, Ohashi N, Umemura K: An Na^+/H^+ exchanger inhibitor suppresses cellular swelling and neuronal death induced by glutamate in cultured cortical neurons. Acta Neurochir [Supple] 86: 223-226, 2003.

Monitoring of singlet oxygen for the experimental photodynamic therapy of the glioma in rats

Summary

Singlet oxygen ($^1O_2$) generated in photodynamic therapy (PDT) plays a very important role to kill the tumor cells. Using a new near infrared-photomultiplier tube (NIR-PMT) system, we monitored the real-time production of $^1O_2$ during PDT and investigated the relationship between the $^1O_2$ production and photodynamic effects. We performed PDT using 5-aminolevulinic acid (ALA), in 9L *in vitro* glioma cells and in rat subcutaneous *in vivo* 9L glioma model. We monitored $^1O_2$ generation using NIR-PMT system, and based on the $^1O_2$ monitoring, we investigated the relation between $^1O_2$ production and photodynamic effects. We could observe the temporal changes of $^1O_2$ production during PDT. At a low fluence rate the $^1O_2$ signal gradually decreased with a low peak, while at a high fluence rate it decreased immediately with a high peak. Consequently, the cumulative $^1O_2$ at a low fluence rate tended to be higher, which induced a strong photodynamic effect. A low fluence rate tended to induce apoptotic change, while a high fluence rate tended to induce necrotic change. The results of this study suggested that the monitoring of $^1O_2$ enables us to predict the photodynamic effect and then allows us to select the optimal laser conditions for each patient.

Keywords:
glioma, 5-aminolevulinic acid (5-ALA), apoptosis, necrosis, photomultiplier

Introduction

Photodynamic therapy (PDT) is very useful for several kinds of cancers. PDT is performed using a photosensitizer, which is selectively taken up and retained by neoplastic tissue. When activated by a laser, the photosensitizer causes direct cell death by generating singlet oxygen ($^1O_2$) (Weishaupt KR et al. 1976; Schweitzer C and Schmidt R 2003). If detecting $^1O_2$ is possible during PDT, we might be able to determine the optimal condition of each photosensitizer. In general, $^1O_2$ generated by PDT undergoes radiant decay, thus resulting in emission at 1270-nm light (Near-infrared luminescence detection) (Krasnovsky AA, Jr. 1998). For the detection of near-infrared luminescence, a new NIR-PMT system (H9170-45, Hamamatsu Photonics K.K., Hamamatsu, Japan) has recently been developed and miniaturized for clinical application. In this study, using a new near infrared-photomultiplier tube (NIR-PMT) system, we monitored the real-time production of $^1O_2$ during PDT with 5-aminolevulinic acid (5-ALA) and investigated the relationship between the $^1O_2$ production and photodynamic effects.

Methods

Monitoring system, and Brain tumor cell lines and animals

Using a new NIR-PMT system (H9170-45, Hamamatsu Photonics K.K., Hamamatsu, Japan), 1270-nm luminescence, which originated from $^1O_2$ through the interfered filter, was collected into the PMT (**Fig. 1**). The photon counts were integrated every 10 and 15 s for 5-ALA-induced protoporphyrin for the *in vitro* and the *in vivo* studies respectively.

9L glioma cells were cultured for several days in RPMI 1640 medium with 10 % fetal calf serum at 37℃ before use. Male Fischer 344 rats (9w) purchased from SLC Inc. (Hamamatsu, Japan) were used for the inoculation of 9L glioma cells.

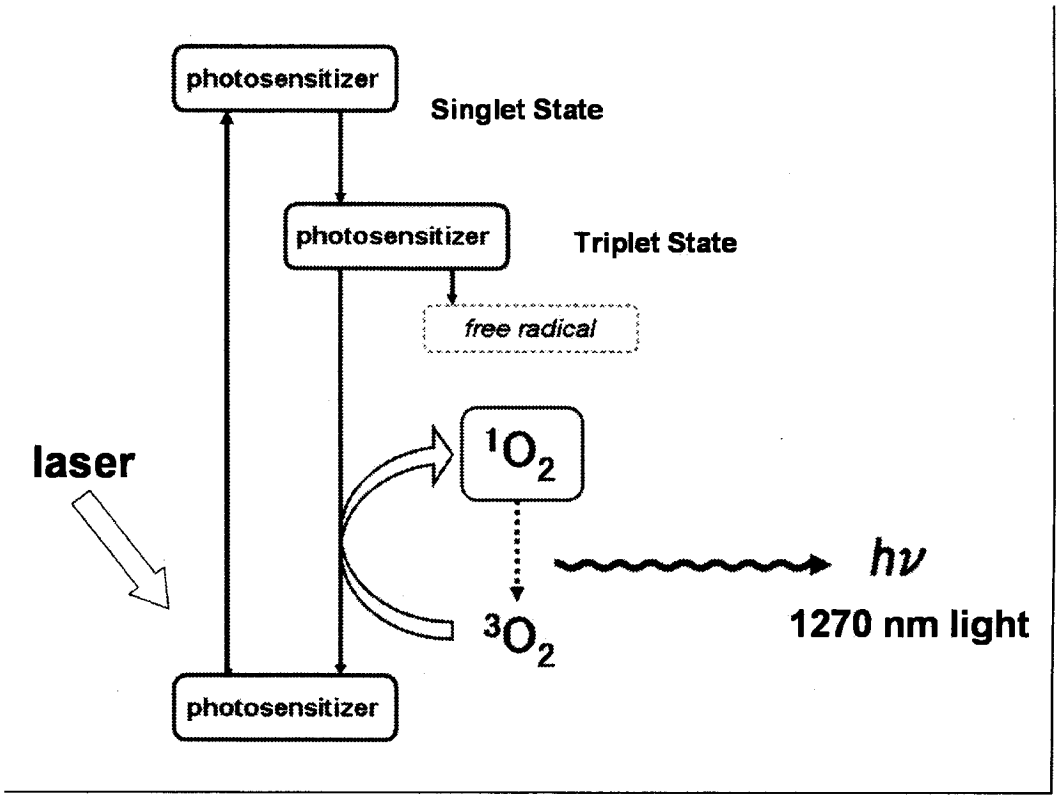

Fig. 1 Principle of the singlet oxygen detection
$^1O_2$ generated by PDT undergoes radiant decay, thus resulting in emission at 1270-nm light Using a new near infrared-photomultiplier tube system (H9170-45, Hamamatsu Photonics K.K., Hamamatsu, Japan), 1270-nm luminescence, which originated from $^1O_2$ through the interfered filter, was collected into the PMT.

Monitoring of $^1O_2$ production in cultured 9L glioma cells

9L glioma cells were incubated with complete medium containing 10 mM 5-ALA for 4 hours. The samples were removed and immediately transferred to the cuvette and measured $^1O_2$ production during PDT. The sample were irradiated at 80 mW/cm^2 (400 s), 160 mW/cm^2 (200 s) and 240 mW/cm^2 (133 s) (n=3). Total fluence was 32 J/cm^2 at each group. After PDT, tumor cells (1×10^4 /well) were seeded in 96-well plates and incubated with fresh medium. The cell viability was determined using the tetrozolium-based colorimetric (MTT) assay at 24 hours after PDT.

Monitoring of the $^1O_2$ production in a rat tumor model

9L glioma cells (1×10^6 cells) were implanted in the skin of rats. 13 days later,

intratumoral irradiation of the subcutaneous tumors was performed (Yamamoto J et al. 2005) at 30 mW/cm (900 s), 60 mW/cm (450 s) and 120 mW/cm (225 s) 4 h after the intravenous administration of 5-ALA (100 mg/kg) (n=6). Total fluence was 27 J/cm at each group.

Thereafter all animals were sacrificed at 48 h after PDT under the deep anesthesia. The tumor tissue specimens were removed and stained with 2,3,5-triphenyltetrazolium chloride (TTC) to determine the tumor death.

Results

Real-time monitoring of $^1O_2$ production during PDT in cultured 9L glioma cells

We could obviously detect the temporal changes of $^1O_2$ production during *in vitro* PDT using NIR-PMT system (**Fig. 2-a,b,c**). Under a fixed fluence, the cumulative $^1O_2$ production increased as the fluence rate decreased **(Fig. 2-d)**. The statistical differences between 80 mW/cm^2 and the other groups were significant **(Fig. 2-d)**.

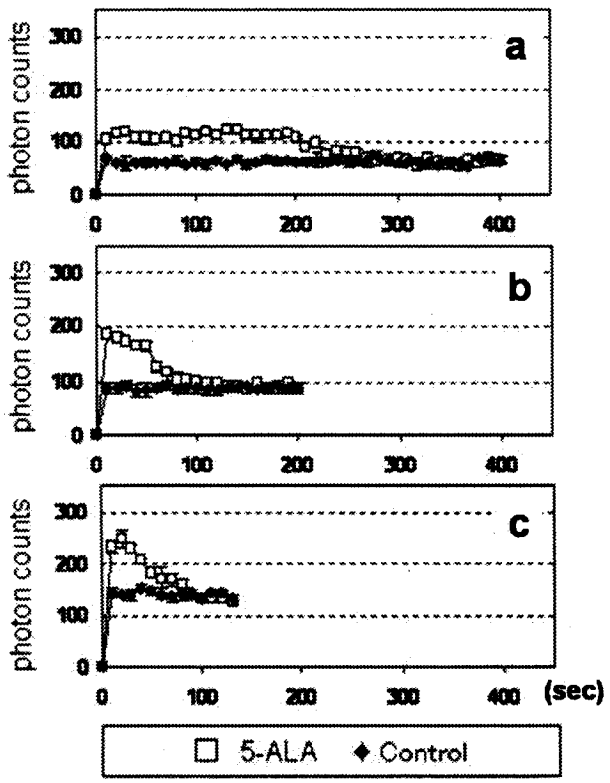

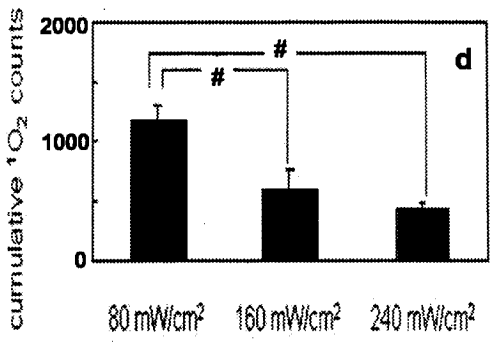

Fig. 2 The temporal changes of $^1O_2$ production in 9L cells during PDT.
9L cells were incubated with 5-ALA (10 mM) for 4 h and exposed to laser light (n=3). The control was incubated without 5-ALA (n=3). Total fluence was 32 J/cm^2. **a)** 80 mW/cm^2 (400 s), **b)** 160 mW/cm^2 (200 s), **c)** 240 mW/cm^2 (133 s). **The cumulative $^1O_2$ counts during PDT at each fluence rate (d)** Note that the cumulative $^1O_2$ production increased as the fluence rate decreased. The data represent the mean ± SE, # $p<0.05$

The cell viability revealed statistical differences between the 5-ALA-treated group and the irradiation alone group at the same irradiance (**Fig. 3**). Although no significant differences were observed among the samples in the irradiation alone group, the differences between 80 mW/cm^2 and the other samples were statistically significant in the 5-ALA-treated group.

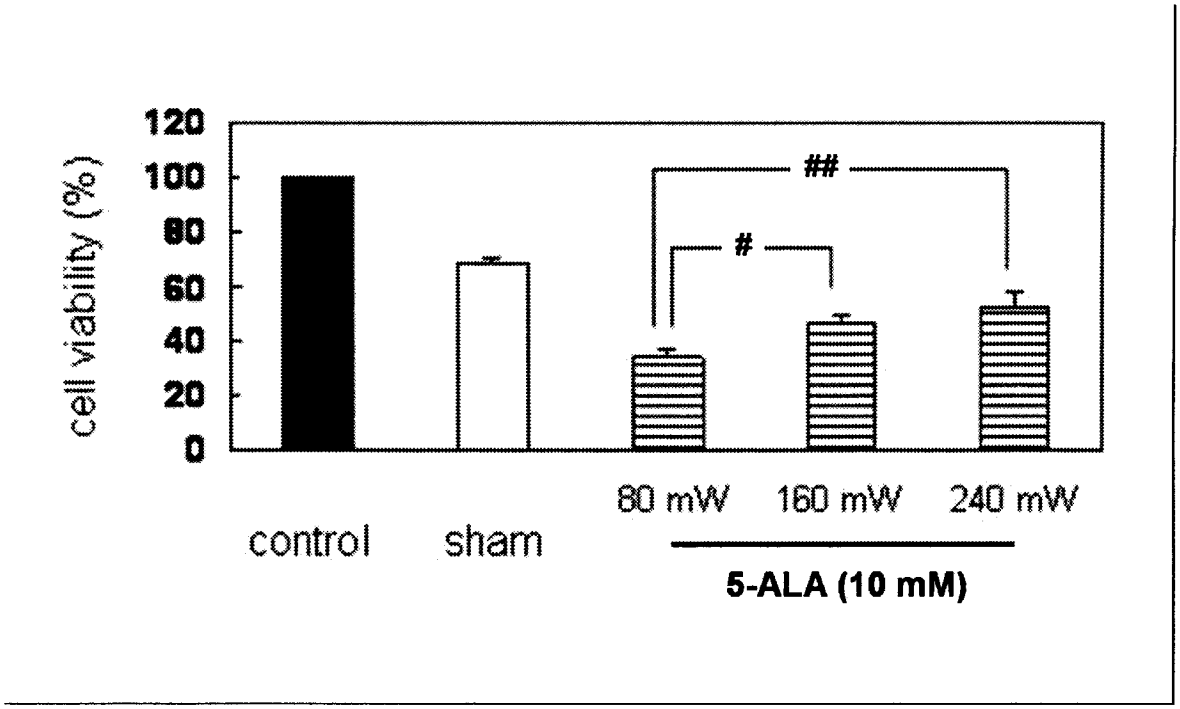

Fig. 3 Cell viability evaluated by an MTT assay
The control group and the sham group were incubated with neither 5-ALA nor light exposure. The sham group was handled as the irradiation was done but without any irradiation (sham irradiation). The data were shown as a percentage of the control value. The data represent the mean ± SE, # $p<0.05$, ##$p<0.01$.

The types of tumor cell death, ie, apoptosis or necrosis, were analyzed by fluorescence imaging using annexin V-FITC and PI staining, fluorescence-based cell death detection. The cell death occurred slowly after PDT in all groups, but the total number and the proportion varied. The majority of cell death in 80 mW/cm^2 (100 s) and 80 mW/cm^2 (200 s) showed early or late apoptosis in any time. On the other hand, the greater part of the cells in 240 mW/cm^2 resulted in necrosis (**Fig. 4**).

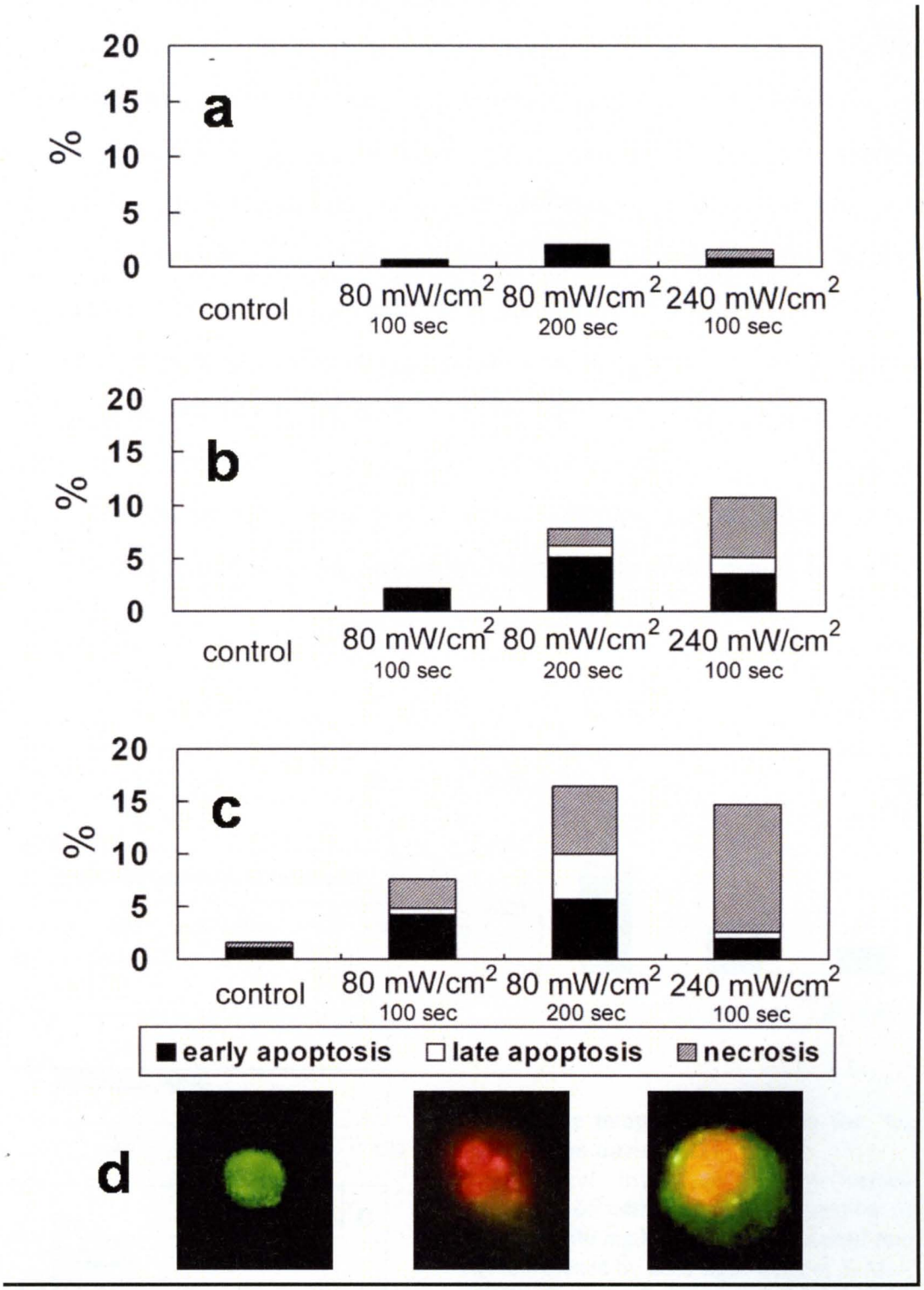

Fig. 4 Proportion of cell death after PDT under different laser conditions
The control was incubated with 5-ALA, but without light exposure. a) 3 h, b) 8 h, c) 24 h after PDT.

Representative images using by annexin V-FITC and PI staining in 9L cells (d)
Left: early apoptotic cell; Note that the cell without swelling was FITC-positive and PI-negative. Center: late apoptotic cell; Note that the cell with fragmentated nucleus was PI-positive. Right: necrotic cell; Note that the swollen cell was FITC- and PI-positive.

Monitoring of $^1O_2$ production in a rat tumor model

The NIR-PMT system could clearly detect the change in $^1O_2$ production during PDT *in vivo* (**Fig. 5a-c**). At a low fluence rate, $^1O_2$ decreased gradually with a low peak, which was comparable to the *in vitro* results. On the other hand, a high fluence rate induced a high peak, but rapidly decreased the $^1O_2$ production. There were no major differences in $^1O_2$ signals between control and 5-ALA-treated samples, especially at the fluence rate of 30 mW/cm and 60 mW/cm. In the animal preparation *in vivo*, the light inside the body may show a lot of scattering and can produce noise detected by NIR-PMT system, inducing the large variation of the data. Although, due to the large variability in the *in vivo* study, the cumulative $^1O_2$ production did not reached the level of statistical differences between the control and 5-ALA-treated samples, they tended to decrease as the fluence rate increased (**Fig. 5d**), which was comparable to the results in the *in vitro* study.

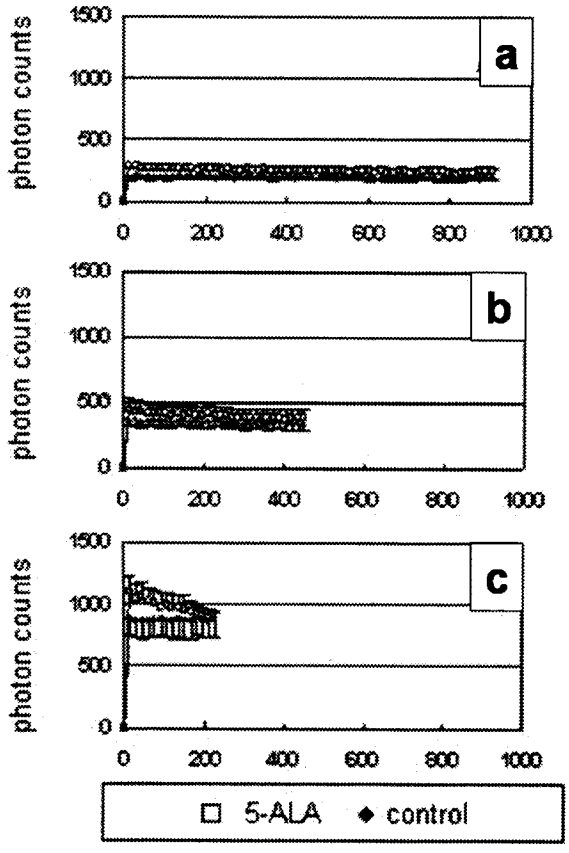

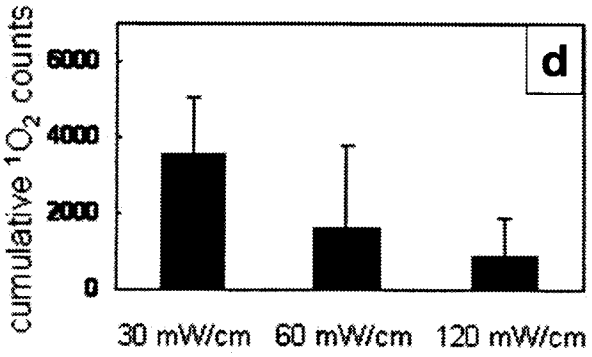

Fig. 5.The temporal changes in the $^1O_2$ production during PDT

Intratumoral irradiation was performed after 4 h of intravenous administration of 5-ALA (100 mg/kg) (n=6). The control rats were exposed by laser light without 5-ALA (n=3). The total fluence was 27 J/cm. **a**) 30 mW/cm (900 s), **b**) 60 mW/cm (450 s), **c**) 120 mW/cm (225 s).

The cumulative $^1O_2$ production during PDT in 5-ALA-treated group (d)

Despite of the same rate of fluence, a difference in the fluence rate revealed different photodynamic effects in experimental tumors (**Fig. 6**). The photodynamic effect in 30 mW/cm group was the strongest (**Fig. 6**). The different types of cell death occurred between 30 mW/cm group and 120 mW/cm group. Though each group showed the apoptotic changes in the boundary zones between the coagulation necrosis and the surviving tumor cells, the number of the apoptotic cells was more in 30 mW/cm group than that in 120 mW/cm group (data not shown). In addition, the TUNEL-positive cells in the former (98%) also significantly ($p<0.01$, $n=6$,) increased in comparison with the latter (68%).

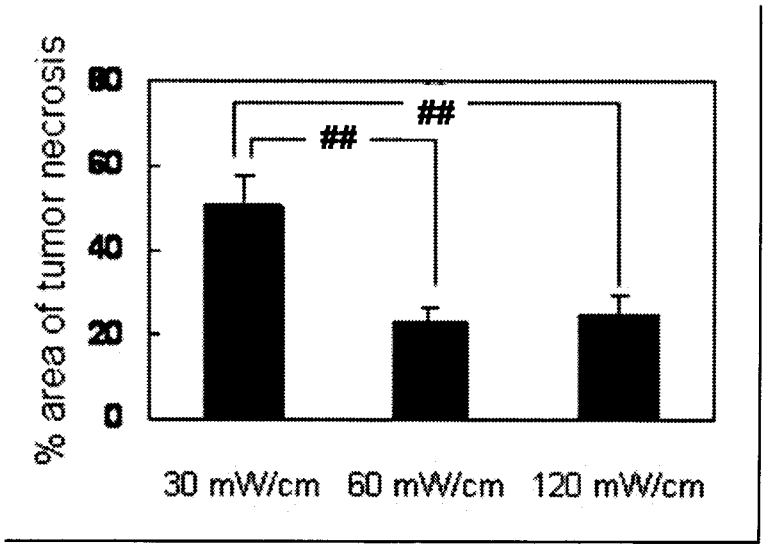

Fig. 6 The photodynamic effect evaluated by TTC stain.
The data were shown as a percentage of the total cross sections in each tissue. The data represent the mean ± SE, ##$p<0.01$.

Comments

We have found that the different condition in laser irradiation varied $^1O_2$ production regarding the peak and decay of the $^1O_2$ signal. During PDT using 5-ALA, the irradiation with a low fluence rate shows a long lasting $^1O_2$ generation. To the contrary, a high fluence rate did not do so. Our results indicated that the optimal condition of irradiation should be decided based on the $^1O_2$ generation.

The laser irradiation after photobleaching is excessive and may damage normal tissue (Powers SK, et al. 1991; Walstad D, et al. 1992; Chen Q, et al. 1996). However,

the duration of irradiation alone cannot predict the occurrence of photobleaching, since the present study also showed that the fluence rate varied the duration that reached the photobleaching. Therefore, the generation of $^1O_2$ should be monitored during PDT. When we monitor the $^1O_2$ production using the detection system and adjust the laser fluence rate or laser pattern (continuous or intermittent) during PDT, it must allow us to perform the appropriate PDT for each patients.

We propose the new NIR-PMT system, used in the present study, to be appropriate for detecting $^1O_2$ signals during PDT. Using this system, we could monitor the $^1O_2$ production during PDT in an experimental tumor model and demonstrated a relationship between the amounts of $^1O_2$ and photodynamic effects. Our new system detects $^1O_2$ production through the optical fiber. Therefore, it can monitor the direct and focal production of $^1O_2$ during PDT *in vitro* and *in vivo*. This miniaturized, desktop-size system must be very useful in a clinical setting.

References

Chen Q, Chopp M, Madigan L, Dereski MO, and Hetzel FW Damage threshold of normal rat brain in photodynamic therapy. Photochem Photobiol 64:163-167, 1996.

Ji Y, Walstad D, Brown JT, and Powers SK Interstitial photoradiation injury of normal brain. Lasers Surg Med 12:425-431, 1992.

Krasnovsky AA, Jr. Singlet molecular oxygen in photobiochemical systems: IR phosphorescence studies. Membr Cell Biol 12:665-690, 1998

Powers SK, Cush SS, Walstad DL, and Kwock L Stereotactic intratumoral photodynamic therapy for recurrent malignant brain tumors. Neurosurgery 29:688-695, 1991.

Schweitzer C and Schmidt R Physical mechanisms of generation and deactivation of

singlet oxygen. Chem Rev 103:1685-1757, 2003

Weishaupt KR, Gomer CJ, and Dougherty TJ Identification of singlet oxygen as the cytotoxic agent in photoinactivation of a murine tumor. Cancer Res 36:2326-2329, 1976

Yamamoto J, Hirano T, Li S, et al. Selective accumulation and strong photodynamic effects of a new photosensitizer, ATX-S10.Na (II), in experimental malignant glioma. Int J Oncol 27:1207-1213, 2005.

INTRAVITAL IMAGING REVEALS THAT TRANSIENT FOREBRAIN ISCHEMIA INDUCES LONG-LASTING INCREASE IN INTRACELLULAR CALCIUM ION CONCENTRATION IN RAT HIPPOCAMPAL CA1

S. Yamamoto, Y. Wang, A. Miyakawa, T. Sakurai, K. Ibaraki, S. Terakawa

Photon Medical Research Center, Hamamatsu University School of Medicine, Hamamatsu, Japan

INTRODUCTION: In cultured neurons, the increase in intracellular Ca^{2+} concentration ($[Ca^{2+}]_i$) plays a crucial role in excitotoxicity. However, in whole animals, calcium response following ischemia remains to be established. Especially, change in $[Ca^{2+}]_i$ in the hippocampus upon ischemia remains unclear, since no method has been available to measure the $[Ca^{2+}]_i$ in the deep structure of brain. In the present study, we sought to determine, in rats, the $[Ca^{2+}]_i$ changes following transient forebrain ischemia in hippocampus.

METHODS: In anesthetized, spontaneously ventilated SD rats (300 g), bilateral vertebral arteries were coagulated, and transient forebrain ischemia was induced by occluding bilateral common carotid arteries with balloon occluders. To obtain the intravital fluorescence image, we employed an imaging fiber bundle (1.0 mm outer diameter) including 20,000 fibers (4.5 μm outer diameter) coupled to the microlens-attached Nipkow-disk scanner (CSU-21, Yokogawa, Japan) equipped with 10x objective lens. This fiber-coupled confocal microscope (FCM) is capable to observe the confocal image just under the fibers (1). FCM was inserted stereotaxically into CA1 and CA3 regions, respectively. Fluo-3/AM (440 μM, 2.5 μl), a $[Ca^{2+}]_i$ sensitive fluorescent dye, was microinjected into the brain, and observed every 30 s before and after 10-min forebrain ischemia with FCM. Since the hemoglobin absorbs both excitation and emission light, ischemia may affect the fluorescent intensity of Fluo-3 inside the brain. To analyze the effects of ischemia on the fluorescence intensity, the fluorescent beads (0.2 μm diameter, similar excitation and emission to those of Fluo-3) were microinjected into hippocampus and the images were taken before and

after 10-min ischemia in the same manner as did in $[Ca^{2+}]_i$ imaging.

RESULTS: Four-vessel occlusion decreased CBF (mean±SD%) measured by laser-Doppler flowmetry, to 25±18 (n=6) in CA1 and to 20±11 (n=6) in CA3. They did not significantly differ. 10-min forebrain ischemia increased fluorescence intensity (mean±SD%) of the beads in the hippocampus up to 108±5 (n=4), which declined to the baseline level following reperfusion. In all measurements, the ischemia showed significant increase (102±2, n=12 to 106±4, n=84, $p<0.01$). In $[Ca^{2+}]_i$ imaging, therefore, the change in fluorescence during ischemia was corrected. During 10-min ischemia, the fluorescence intensity of Fluo-3 slightly increased up to 110±9, and then increased to 134±19 at the end of 20-min reperfusion in CA1 (n=4). In contrast, in CA3 (n=5), the intensity did not change upon ischemia, and at reperfusion slightly elevated to 108±4 without long-lasting increase. During 14-20 min reperfusion, the $[Ca^{2+}]_i$ increase in CA1 was statistically larger ($p < 0.05$) than that in CA3.

COMMENTS: In CA1, but not in CA3, transient forebrain ischemia induced long lasting Ca^{2+} increase *in situ*, whereas it produced similar CBF changes in these regions. Since the $[Ca^{2+}]_i$ increase was significantly larger in CA1 during reperfusion period, it might reach to toxic levels and then mediate the vulnerability of CA1 against ischemia.

REFERENCES

1) Sakurai T, Yamamoto S, Miyakawa A, et al. (2006) Fiber-coupled confocal microscope (FCM) for real time imaging of cellular signals in vivo. *Proc of SPIE* 6088:608803-1 - 608803-6.

Presented by S. Yamamoto (Oral Presentation) in the 23rd International Symposium on Cerebral Blood Flow, Metabolism & Function (Brain'07) and the 8th International Conference on Quantification of Brain Function with PET (BrainPET'07) which was held in Osaka on May 20-24, 2007.

ALPHA-AMINO-3-HYDROXY-5-METHYL-4-ISOXAZOLE PROPIONIC ACID (AMPA) RAPIDLY INDUCES DNA FRAGMENTATION OF THE HIPPOCAMPAL NEURONS IN THE INITIAL STAGE OF NECROSIS

K. Ibaraki, S. Yamamoto, Y. Wang, A. Miyakawa, T. Sakurai, S. Terakawa

Photon Medical Research Center, Hamamatsu University School of Medicine, Hamamatsu, Japan

INTRODUCTION: Under the video enhanced contrast-differential interference contrast (VEC-DIC) microscope, the intact cultured neurons show large nuclei containing an amorphous nucleoplasm, and an application of glutamate induces granular structure inside the nucleus within 20 minutes (1). This nuclear change corresponds to DNA fragmentation, indicating that the extracellular stimuli would affect the nuclear DNA in the very early stage of excitotoxicity (2). However, whether alpha-amino-3-hydroxy-5-methyl-4-isoxazole propionic acid (AMPA) could produce the comparable change remains unclear. In the present study, we sought to determine the sole effects of AMPA application on the hippocampal neurons.

METHODS: Dissociated hippocampal cultures were prepared from one-day old Wister rats, and used for the experiment three weeks later. Morphological changes in hippocampal neurons induced by AMPA were observed under the VEC-DIC microscope. To detect the type of cell death, that is, necrosis or apoptosis, hippocampal neurons were stained following AMPA application with propidium iodide (PI) and fluorescein-4-isothiocyanate (FITC) conjugated annexin V (annexin V-FITC), and examined under the fluorescence microscope. DNA fragmentation was assessed using comet assay, a single cell gel electrophoresis assay. To assess the severity of DNA fragmentation, we classified DNA damage from grade 1 (no damage) to 5 (severe damage) by visual scoring.

RESULTS: Under the VEC-DIC microscope, continuous exposure to higher concentration of AMPA (100 μM, 1 mM) dose-dependently showed the nuclear

granulation and the cellular swelling within 5 minutes. Although 10 μM-AMPA also induced the cellular swelling, it did not produce the marked nuclear granulation, suggesting that the pathway inducing cellular swelling may be distinct from that inducing nuclear granulation. Non-competitive AMPA receptor antagonist, GYKI-52466 (50 μM), blocked these morphological changes after continuous exposure to 100 μM-AMPA for 1 h, while N-methyl-D-aspartate (NMDA) receptor blocker, MK-801 (20-200 μM), did not do so, indicating that AMPA mediated toxicity independently of NMDA receptor activation. The staining with PI and annexin V-FITC revealed that AMPA (100 μM, 1 mM) induced necrosis but not apoptosis in dose dependent manner. The treatment with AMPA (100 μM, 1 mM) for 1 h significantly increased the percentage of grade 4, severer DNA fragmentation in comet assay.

COMMENTS: In hippocampal neurons, AMPA receptor stimulation alone, independently of NMDA receptor, induces the cellular swelling and the nuclear granulation in the very early stage of necrosis. The granular change in the nucleus observed under the VEC-DIC microscope corresponds to DNA fragmentation. Our results suggest that: 1) even in the process of necrosis, the extracellular stimuli to the AMPA receptor rapidly produce the nuclear signal to induce DNA fragmentation; and 2) the pathway inducing DNA fragmentation may be less sensitive to AMPA receptor activation as compared with that inducing cellular swelling.

REFERENCES

1) Ikeda J et al. (1996) Nuclear disintegration as a leading step of glutamate excitotoxicity in brain neurons. J Neurosci Res 43: 613-622.

2) Yamamoto S et al. (2003) Excitotoxic signal rapidly induces random DNA fragmentation through inositol trisphophate pathway. J Cereb Blood Flow Metab 23 (Suppl): 338.

Presented by K. Ibraki (Poster Presentation) in the 23rd International Symposium on Cerebral Blood Flow, Metabolism & Function (Brain'07) and the 8th International Conference on Quantification of Brain Function with PET (BrainPET'07) which was held in Osaka on May 20-24, 2007.

OXYGEN RADICAL PRODUCTION IN RAT ISCHEMIC BRAIN MEASURED BY INTRAVITAL FLUORESCENCE IMAGING

Yong Wang, Seiji Yamamoto, Atsuo Miyakawa, Takashi Sakurai, Kyoko Ibaraki, Susumu Terakawa

Photon Medical Research Center, Hamamatsu University School of Medicine, Hamamatsu, Japan

INTRODUCTION: Several studies using electron-spin resonance showed increased oxygen free radical formation during ischemia. However, the results remain controversial. In the present study, to analyze the controversial issue, we tried to establish a new semi-quantitative analysis system that could spatiotemporally detect the cortical intracellular oxygen radical changes of adult rat brain, and sought to determine how the production of oxygen radicals could change in ischemia-reperfusion.

METHODS: Adult male SD rats (300 g) were anesthetized and spontaneously ventilated. After instrumentation, bilateral vertebral arteries were coagulated, and transient (10 min) forebrain ischemia was induced by occluding bilateral common carotid arteries with balloon occluders. The regional cerebral blood flow (rCBF) was measured by laser-Doppler flowmetry. To observe the oxygen radical production, cranial window was made over the frontal cortex, and a fluorescent dye (2.5 μl) was microinjected to the cortical region. To measure superoxide radical ($\cdot O_2^-$) production, MitoSOX Red (5μM, Molecular Probes), a fluorescent dye for mitochondrial $\cdot O_2^-$, was used, and to measure hydroxyl radical (·OH) production, Hydroxyphenyl Fluorescein (20 μM, Daiichi Pure Chemicals, Japan), a fluorescent ·OH indicator, was used. After microinjection, closed cranial window was made over the cortex, and the fluorescence images were taken under a microscope (BX50WI, Olympus) equipped with a confocal scanner of a microlens-attached Nipkow-disk (CSU-21, Yokogawa, Japan) every 30 s before and after 10-min ischemia. The free radical scavenger, edaravon (3-methyl-1-phenyl-2-pyrazolin-5-one, Mitsubishi Pharma Corporation, Japan), which has been developed as a neuroprotective agent, is approved for the treatment of acute

cerebral infarction in Japan. To test the feasibility of our intravital imaging system, edaravon (3.0 mg/kg) was intravenously injected 5 min before ischemia, and measured $\cdot O_2^-$ and ·OH.

RESULTS: Mean arterial pressure and blood gases were within normal limits for anesthetized rats, and did not differ among the groups. In the control animals without ischemia, $\cdot O_2^-$ and ·OH did not significantly increase (n=3/each). During 10-min ischemia, the rCBF (mean±SD) dropped to 29±7% (n=6). The $\cdot O_2^-$ production (n=5) began to significantly increase at the 5 min after the onset of ischemia, reached to 160±13% at the end of ischemia, and persistently increased up to 186±20% during 20-min reperfusion. The ·OH production (n=5) started to increase at the 5 min after the onset of ischemia, elevated to 131±12% at the end of ischemia, and persistently increased up to 183±10% during reperfusion. The treatment with edaravon completely scavenged ·OH to the control level ($p<0.01$, n=3), but did not do so in $\cdot O_2^-$ generation (n=5).

COMMENTS: In the present study, the intravital imaging indicated that $\cdot O_2^-$ and ·OH production increased in the ischemia and reperfusion in rats. Whereas ischemia (ischemic rCBF=30%) produced oxygen radicals, reperfusion strongly enhanced the production. Especially, during reperfusion, production of ·OH, toxic reactive oxygen species, was more than $\cdot O_2^-$. Our system allows us to observe real-time production of oxygen radicals, which is useful for investigating the pathological roles of free radical in the brain.

Presented by Y. Wang (Poster Presentation) in the 23rd International Symposium on Cerebral Blood Flow, Metabolism & Function (Brain'07) and the 8th International Conference on Quantification of Brain Function with PET (BrainPET'07) which was held in Osaka on May 20-24, 2007.